

**SOME ASPECTS OF PERFORMANCE APPRAISAL
OF ALUMINIUM–SILICON CARBIDE PARTICULATE
(SiCp) METAL MATRIX COMPOSITE**

**A THESIS IN PARTIAL FULFILMENTS OF REQUIREMENTS
FOR THE AWARD OF THE DEGREE OF
Master in Technology (Research)**

Archived in Dspace@NITR

<http://dspace.nitrkl.ac.in/dspace>

SOME ASPECTS OF PERFORMANCE APPRAISAL OF ALUMINIUM–SILICON CARBIDE PARTICULATE (SiCp) METAL MATRIX COMPOSITE

**A THESIS IN PARTIAL FULFILMENTS OF REQUIREMENTS
FOR THE AWARD OF THE DEGREE OF
Master in Technology (Research)**

Submitted to

NATIONAL INSTITUTE OF TECHNOLOGY, ROURKELA

BY

**SANJIBANI PANI
(ROLL NO. – 60404001)**

Under the Supervision of

**Dr. U.K. Mohanty (Professor)
&
Dr. S.C. Mishra (Professor)**



**DEPARTMENT OF METALLURGICAL & MATERIALS ENGINEERING
NATIONAL INSTITUTE OF TECHNOLOGY
ROURKELA – 769 008
INDIA**

CERTIFICATE

This is to certify that the Thesis entitled “Some Aspects of Performance Appraisal of Aluminium – Silicon Carbide particulate (SiC_p) Metal-matrix Composites” submitted by Mrs. Sanjibani Pani, Deptt. of MME, N.I.T. Rourkela, as a partial fulfillment of requirements for the award of the Degree of Master In Technology (Research) has been carried out under our supervision and has not been submitted elsewhere fancy award of any degree.

*Dr. S. C. Mishra
Prof. MME. Deptt.*

*Dr. U. K. Mohanty
Prof. MME. Deptt.*

Acknowledgement

It gives me immense pleasure to take this opportunity to express my sincere and heart felt thanks to Prof.U.K.Mohanty and Prof. S.C. Mishra of the Dept of Metallurgical and Materials Engg, National Institute of Technology, Rourkela for their able and continual guidance and help through out the entire period of investigation. Their never-ending inspiration and unfailing encouraging words have been the key to completion of this thesis.

I take this opportunity to thank Dr. B.C.Ray, Professor M M Engg Dept. for his inspiration and timely technical advice, whenever I needed, without hesitation. I have no hesitation to admit that but for his active cooperation this thesis could not have seen light.

My sincere thanks are also due to Mr.Uday Kumar Sahu, Mr.Rajesh Pattnaik, and Mr. Sameer Pradhan who have helped me to a very great extent, even in Institute off-days and off-hours, to conduct various related experiments for a meaningful completion of this thesis.

I thank Prof. G.S. Agarwal, HOD MM Engineering, Department for his kind support and valuable advice for the completion of the thesis.

Lastly, I take this opportunity to express my heartfelt regards and sincere thanks to my family member for their timely support and encouragement, which encouraged me a great deal in completing the thesis and put it in black and white.

Sanjibani Pani

CONTENTS

CHAPTER	TITLE	PAGE NO
1	INTRODUCTION	1
2	LITERATURE SURVEY	
	2.1 Introduction	7
	2.2 Metal Matrix Composite	8
	2.3 Al-SiC MMCs	12
	2.4 Processing of Metal Matrix Composite	17
	2.4.1 Liquid state processing of MMCs	18
	2.4.1.1 Infiltration Processes	19
	2.4.1.1.1 No External Force	20
	2.4.1.1.2 Vacuum Driven Infiltration	20
	2.4.1.1.3 Pressure Driven Infiltration	21
	2.4.1.1.4 Other Forces	21
	2.4.1.2 Dispersion Processes	22
	2.4.1.3 Spray Processes	23
	2.4.1.4 In Situ Process	24
	2.4.2 Solid-State processing of MMCs	25
	2.4.3 Primary solid state processing of discontinuously reinforced composite	25
	2.4.3.1 Powder Blending and Consolidation	25
	2.4.3.2 Mechanical Alloying	26
	2.4.3.3 Diffusion Bonding or Roll Bonding	27
	2.4.3.4 High Rate Consolidation	27
	2.4.3.5 Powder Coating followed by solid-state consolidation.	28
	2.5 Deformation Processing of Metal-Matrix Composites.	30
	2.5.1 Extrusion of consolidated MMCs	30
	2.5.2 Rolling of consolidated MMCs.	31
	2.5.3 Forging of consolidated MMCs.	31
	2.6 A Bird's Eye-view of the Literature surveyed	32
	2.7 Conclusions	38
3	EXPERIMENTAL	
	3.1 Introduction	39
	3.2 Equipment/Instruments Used	39
	3.3 Equipment / Instruments used in the Present Investigation	
	3.4 Selection and characterization of Raw Materials	40
	3.4.1 Aluminium Metal Powder	42

3.4.2	SiC Particulates	42
3.4.3	Pre-treatment of SiC Particulates	42
3.5	Fabrication of the green Test Specimen	49
3.5.1	Mixing of the powders	49
3.5.1.1	Optimisation of mixing time	49
3.5.2	Compaction of the powder mixing	49
3.5.2.1	Cold Uniaxial pressing	51
3.5.2.2	Cold Isostatic Pressing	51
3.5.3	Sintering of the green pellets	51
3.5.3.1	Nomenclature of the test specimens	51
3.5.4	Drilling of the sintered test pieces	52
3.6	Exposure of the test specimen to thermal shock	53
3.7	Determination the radial crushing strength	53
3.8	Scanning Electron Microscopy	54
3.9	Conclusion	55
4	RESULTS & DISCUSSION	
4.1	Introduction	56
4.2	Assessment and Evaluation based by Mechanical Testing.	56
4.2.1	Load at rupture under thermal shock	56
4.2.2.	Stresses at rupture under thermal shock	63
4.2.3.	Displacement at rupture under thermal shock	67
4.2.4	Strain at rupture due to thermal shock	72
4.2.5	Radial crushing strength under thermal shock.	76
4.3	Assessment and Evaluation based on SEM Micrograph.	79
5	CONCLUSIONS	85
•	BIBLIOGRAPHY	86

LIST OF TABLES

Table No.	Title	Page No.
1	A birds Eye-view of the literature surveyed	32
2	List of the equipment/instruments used in the present investigations.	40
3	Load values at rupture	56
4	Stress values at rupture	63
5	Displacement values at rupture	67
6	Strain values at rupture	72
7	Radial crushing strength values	76

LIST OF FIGURES

Figure No.	Title	Page No.
1	Particle Size Analyser	43
2	Planetary Ball Mill	43
3	X-ray Diffractometer	44
4	Image Analyzer	44
5	Cold Uniaxial Hydraulic Press	45
6	Cold Isostatic press	45
7	High Temperature Horizontal Tubular furnace	46
8	Drilling M/c	46
9	Electric Oven	47
10	Cryogenic Chamber	47
11	Instron 1195	48
12	Scanning Electron Microscope	48
13	2 hrs mixing of Al & SiC powders	50
14	4 hrs mixing of Al & SiC powders	50
15	6 hrs mixing of Al & SiC powders	50
16	8 hrs mixing of Al & SiC powders	50
17	A sintered test specimen	53
18	A drill test specimen	53
19	Experimental arrangement showing the holding of the ring shaped specimen.	54
20	A sintered specimen before drilling	56
21	A fractured specimen after the compression test.	56
22	Load at rupture Vs Temperature as a function of Time (Exposed to +80 ⁰ C)	57
23	Load at rupture Vs Temperature as a function of Time (Exposed to -80 ⁰ C)	57
24	Load at rupture Vs time at sintering temperature for samples exposed to +80 ⁰ C and -80 ⁰ C (Sintering Temp. 600 ⁰ C)	58
25	Load at rupture Vs time at sintering temperature for samples exposed to +80 ⁰ C and -80 ⁰ C (Sintering Temp. 580 ⁰ C)	58

26	Load at rupture Vs time at sintering temperature for samples exposed to +80 ⁰ C and –80 ⁰ C (Sintering Temp. 560 ⁰ C)	58
27	Load at rupture Vs time at sintering temperature for samples exposed to +80 ⁰ C and –80 ⁰ C (Sintering Temp. 540 ⁰ C)	58
28	Stress at rupture Vs Temperature as a function of Time (Exposed to +80 ⁰ C)	64
29	Stress at rupture Vs Temperature as a function of Time (Exposed to -80 ⁰ C)	64
30	Stress at rupture Vs time at sintering temperature for samples exposed to +80 ⁰ C and –80 ⁰ C (Sintering Temp. 600 ⁰ C)	65
31	Stress at rupture Vs time at sintering temperature for samples exposed to +80 ⁰ C and –80 ⁰ C (Sintering Temp. 580 ⁰ C)	65
32	Stress at rupture Vs time at sintering temperature for samples exposed to +80 ⁰ C and –80 ⁰ C (Sintering Temp. 560 ⁰ C)	65
33	Stress at rupture Vs time at sintering temperature for samples exposed to +80 ⁰ C and –80 ⁰ C (Sintering Temp. 540 ⁰ C)	65
34	Displacement at rupture Vs Temperature as a function of Time (Exposed to +80 ⁰ C)	67
35	Displacement at rupture Vs Temperature as a function of Time (Exposed to -80 ⁰ C)	68
36	Displacement at rupture Vs time at sintering temperature for samples exposed to +80 ⁰ C and –80 ⁰ C (Sintering Temp. 600 ⁰ C)	68
37	Displacement at rupture Vs time at sintering temperature for samples exposed to +80 ⁰ C and –80 ⁰ C (Sintering Temp. 580 ⁰ C)	68
38	Displacement at rupture Vs time at sintering temperature for samples exposed to +80 ⁰ C and –80 ⁰ C (Sintering Temp. 560 ⁰ C)	68
39	Displacement at rupture Vs time at sintering temperature for samples exposed to +80 ⁰ C and –80 ⁰ C (Sintering Temp. 540 ⁰ C)	68
40	Strain at rupture Vs Temperature as a function of Time (Exposed to +80 ⁰ C)	72
41	Strain at rupture Vs Temperature as a function of Time (Exposed to -80 ⁰ C)	73
42	Strain at rupture Vs time at sintering temperature for samples exposed to +80 ⁰ C and –80 ⁰ C (Sintering Temp. 600 ⁰ C)	73
43	Strain at rupture Vs time at sintering temperature for samples exposed to +80 ⁰ C and –80 ⁰ C (Sintering Temp. 580 ⁰ C)	73

44	Strain at rupture Vs time at sintering temperature for samples exposed to +80 ⁰ C and –80 ⁰ C (Sintering Temp. 560 ⁰ C)	73
45	Strain at rupture Vs time at sintering temperature for samples exposed to +80 ⁰ C and –80 ⁰ C (Sintering Temp. 540 ⁰ C)	73
46	Radial Crushing Strength Vs Temperature as a function of Time (Exposed to +80 ⁰ C)	76
47	Radial Crushing Strength Vs Temperature as a function of Time (Exposed to -80 ⁰ C)	77
48	Radial Crushing Strength Vs time at sintering temperature for samples exposed to +80 ⁰ C and –80 ⁰ C (Sintering Temp. 600 ⁰ C)	77
49	Radial Crushing Strength Vs time at sintering temperature for samples exposed to +80 ⁰ C and –80 ⁰ C (Sintering Temp. 580 ⁰ C)	77
50	Radial Crushing Strength Vs time at sintering temperature for samples exposed to +80 ⁰ C and –80 ⁰ C (Sintering Temp. 560 ⁰ C)	77
51	Radial Crushing Strength Vs time at sintering temperature for samples exposed to +80 ⁰ C and –80 ⁰ C (Sintering Temp. 540 ⁰ C)	77

LIST OF MICROGRAPHS

Micrograph No.	Title	Page No.
1	Temp – 600 ⁰ C, Time – 1.5hrs, Treatment – “-80 ⁰ C”	81
2	Temp – 560 ⁰ C, Time – 1.5hrs, Treatment – “-80 ⁰ C”	81
3	Temp – 540 ⁰ C, Time – 1hr, Treatment – “-80 ⁰ C”	81
4	Temp – 540 ⁰ C, Time – 2hrs, Treatment – “-80 ⁰ C”	81
5	Temp – 560 ⁰ C, Time – 1.5hrs, Treatment – “-80 ⁰ C”	81
6	Temp – 580 ⁰ C, Time – 1hr, Treatment – “+80 ⁰ C”	83
7	Temp – 560 ⁰ C, Time – 1hr, Treatment – “+80 ⁰ C”	83
8	Temp – 580 ⁰ C, Time – 1hr, Treatment – “-80 ⁰ C”	83
9	Temp – 540 ⁰ C, Time – 2hrs, Treatment – “-80 ⁰ C”	83
10	Temp – 600 ⁰ C, Time – 2hrs, Treatment – “-80 ⁰ C”	83

ABSTRACT

Stresses induced due to thermal mismatch between the metal matrix and the ceramic reinforcement in metal matrix composite may impart plastic deformation to the matrix thereby resulting in a reduction of the residual stresses. Thermal mismatch strains also may quite often crack the matrix resulting in a relaxation of the residual stresses.

The interface in MMCs is a porous, non-crystalline portion in comparison with the matrix or the reinforcement (metal matrix and ceramic reinforcement in this case). Therefore residual stresses are readily released at the porous and non-crystalline interface as a result of which when particle density is high, i.e. in regions which are particle starved, meaning the availability of the interface is limited, particle fracturing is predominating.

In the present investigation ring-shaped Al-SiCp MMCs are fabricated in the solid state processing route. The sintering temperature and time of holding at the sintering temperature are varied and the samples are subjected to thermal shock at $+80^{\circ}\text{C}$ and at -80°C in different batches. The radial crushing strength of the specimens are determined using Instron-1195 adopting standard test methods. Extensive micrographs of the fractured surfaces are analyzed.

Assessment and evaluation on the basis of mechanical properties reveal that thermal shock due to a sub-ambient temperature is more damaging compared to that due to an exposure to an elevated temperature.

The micrographs studies reveal that in general when the thermal shock is due to the exposure to an elevated temperature, the dominating failure mode is cavity generation at the interface, i.e. nucleation and coalescence of voids for the formation and propagation of cracks at interface region leading to final failure. The micrographs further reveal that in the case of a thermal shock caused due to exposure to a sub-ambient temperature, the dominating failure mode is due to interfacial failure/or matrix damage.

CHAPTER 1

INTRODUCTION

INTRODUCTION

The human quest for finding a material tailor-made to perform under specified environmental conditions is never ending. This has prompted researchers to enhance their research work for addressing to the materials need of the ever expanding and ever challenging human world. It is well known in the materials world that one can create new materials with unique properties, which can be tailor-made and are different from their constituent ingredients [1]. This very concept is responsible for creating composite materials of various types with a matrix that is strengthened by the reinforcement it contains. It is needless to say, neither the matrix nor the reinforcement can singularly possess the characteristic resulting properties of the composite, of which they are the constituents and that the composite can be tailor-made to perform in varying ambient conditions satisfactorily by adopting different processes for fabrication using varying proportions of the matrix and the reinforcement and even by changing either type of the matrix or the reinforcement or both of them.

Metal Matrix Composites (MMCs) have emerged as a class of material capable of advanced structural, aerospace, automotive, electronic, thermal management and wear applications. The MMCs have many advantages over monolithic metals including a higher specific modulus, higher specific strength, better properties at elevated temperatures, lower coefficients of thermal expansion and better wear resistance. However, on the debit side, their toughness is inferior to monolithic metals and they are more expensive. In comparison with most polymer-matrix composites (PMCs). MMCs have certain superior mechanical properties namely higher transverse strength and stiffness, greater shear and compressive strength and better high temperature

capabilities. In addition to this, some of the physical attributes of MMCs such as no significant moisture absorption properties, non inflammability, high electrical and thermal conductivities and resistance to most radiations, have made these materials active subjects of scientific investigation and applied research [2].

MMCs in general, consist of at least two components, the metal matrix and the reinforcement. In all cases the matrix is defined as a metal, but pure metal is rarely used; it is generally an alloy. The two most commonly used metal matrices are based on Aluminium and Titanium. Both of these metals have comparatively low specific gravities and are available in a variety of alloy forms. Although Magnesium is even lighter, its great affinity for oxygen promotes atmospheric corrosion and makes it less suitable for many applications. Beryllium is the lightest of all structural metal and has a tensile modulus higher than that of steel. However, it suffers from extreme brittleness, which is the reason for its exclusion as one of the potential matrix material. Nickel and Cobalt based super alloys have also been used as matrices, but the alloying elements in these materials tend to accentuate the oxidation of fibres at elevated temperatures. MMCs reinforcement can be generally divided into five major categories; continuous fibres, discontinuous fibres, whiskers, wires, and particulates (including platelets). With the exception of wires, which are metals, reinforcements are generally ceramics. Typically these ceramics are oxides, carbides and nitrides that are used because of their excellent combination of specific strengths and stiffness at both ambient as well as elevated temperatures.

Aluminum and its alloys have the most attention, as matrix materials for MMCs and the most common reinforcement is SiC. Aluminum (commercially pure having an

assay of 99% of Aluminum) and SiC particulates have been used for the MMC fabrication in the present investigation.

Metal Matrix Composites, alternatives to conventional materials, provide the specific mechanical properties necessary for elevated as well as ambient temperature applications. The performance advantages of these materials include their tailored mechanical, physical and thermal properties in light of their low density, high specific modulus, high strength, high thermal conductivity, good fatigue response, control of thermal expansion, high abrasion and wear resistance, etc. Some of the typical applications of MMCs include their use in fabrication of satellite, missile, helicopter structures, structural support, piston, sleeves and rims, high temperature structures, drive shaft, brake rotors, connecting rods, engine block liners various types of aerospace and automotive applications etc. [3].

However, it must be clearly under-stood and appreciated that though a ductile metal matrix (such as Aluminium) when impregnated by a significant volume fraction of a stiff nonmetallic phase (such as silicon carbide) results in phenomena that are specific to reinforced metals, the associated issues that need to be addressed to and answered satisfactorily are the following:

Interfacial bonding between the reinforcement and the matrix, Residual stresses,

Matrix dislocations generated by the thermal mismatch between phases and Reinforcements and alterations in matrix precipitation kinetics.

The performance limits of metal matrix composites can be raised by addition of a high volume fraction of whiskers or particulate. An example is the development of aluminium metal matrix composites by mixing and consolidating aluminium powder and high modulus, low density, micron and sub micron sized carbides such as SiC. With the additions of refractory SiC particulate and /or whiskers, the strength modulus and wear resistance of the resulting MMC increases. However, this increase is accompanied by a reduction of ductility and fracture toughness. Thus the additional constituents result in both desirable and detrimental changes to the mechanical and physical characteristic properties of the MMC being developed, [4].

It is in this context that the present investigation has been taken up in pure scientific interest to evaluate the desirable as well as detrimental effect of the reinforcement provided by SiC particulates to commercially pure Al (99% + Al) which has good ductility and formability. (It is well understood that the experimental data has little relevance in the practical / industrial arena, nevertheless the data can be used as a platform for carrying but further experimentation with different Aluminum alloys reinforced with SiC particulates. In the present investigation SiCp reinforced Al (99% + Al) MMCs are fabricated adopting the solid-state processing route i.e. mixing and consolidations Al, metal powder and SiC particulates. The sintering temperature and time at temperature are varied. The test piece are exposed to + 80⁰C and – 80⁰ C in different catches. Radial crushing strength 'k' of the treated samples are calculated in line with the provisions of the ASTM committee B 09 the metal powders and metal powder products with the data obtained using Instron 1195. The stress, strain and the displacement parameters if the samples are related at the maximums load. These

experimental data and the calculated values are tabulated and vividly analyzed for different sintering temperatures and time at temperature by plotting the related bar charts, graphs, etc.

The microphotographs of the fractured surfaces of the samples as obtained through Scanning Electron Microscope are extensively examined. An attempt is made to interpret the experimental data obtained on the basis of the micrographs. The interfacial bonding, residual stresses generated and matrix dislocations generated as a consequence of thermal mismatch have been especially brought under focus to explain experimental observations.

This report contains five numbers of distinct chapters. The 1st chapter, 'Introduction' attempts to give an insight to the work under taken and highlights the procedure adopted in the completion of the investigation.

The 2nd chapter on 'Literature Survey' is dedicated to an extensive survey of the work carried out by other investigators /agencies in the field. The help of work carried out by these workers has been referred to wherever necessary to explain and support the present experimental findings.

The 3rd chapter, 'Experimental Design' is devoted to explain the experimental procedure adopted in the present investigation along with the experimental arrangements and details of experiments carried out. The instruments/ apparatus and the prescribed experimental norms as adopted in the present investigations have been explained in details.

The 4th chapter houses the results in the form of tables, graphs, bar-diagrams, SEM – micrographs etc. which have been generated while carrying out the investigations. This also houses a detailed discussion of the results made on the basis of the experimental data.

Finally, on the basis of the experimental findings some useful conclusions have been provided in the 5th and the last chapter.

CHAPTER 2

LITERATURE SURVEY

2.1 Introduction

The term composite could mean almost anything if taken at face value, since all materials are comprised of dissimilar sub-units when examined at closed enough details. In modern materials engineering, the term usually, refers to a matrix- material that is reinforced by a material with high strength, stiffness and modulus that serves as the principal load-carrying component of the composites. Many composites used today are at the leading edge of materials technology with performance and costs justifying their ultra demanding applications.

The reinforcements used in modern composites have strength and stiffness far above the traditional materials. These may be in the shape of fibres, whiskers or even particulates. The fibre- reinforced- polymer composites (FRPs) have found wide spread applications as a group of important structural materials over their metallic counter parts [5]. The reinforcement materials, say fibres, are not usable as fibre alone and typically they are contained in the matrix material that acts to transfer load to the fibre i.e., the reinforcement. The matrix also protects the fibres from abrasion and environmental attack. The matrix is generally more ductile than the fibre and the source of composite toughness [6]. The light- weight and high specific strength and modulus of the composite materials have allowed them, the FRP composites, to break into major markets in automotive construction and aeronautics- industries. In fact NASA have declared their intent to build a 100% composite aircraft by 2010, [7].

Fibre reinforced polymeric composite materials (FRPs) offer many advantages over conventional structural materials. They have high strength and modulus-to-weight ratio, are fatigue and corrosion resistant, tailor-made and require low maintenance. However, the polymer matrix composites suffer from some physical characteristic properties such as significant moisture absorption properties giving rise to high residual stresses, high inflammability, low electrical and thermal conductivities and low resistance to most radiations. In view of the above the MMCs have been developed which can be tailor-made to suit a specific use yet don't suffer from the deficiencies that the polymer matrix composites suffer from.

2.2 Metal Matrix Composites (MMCs)

Composites materials, as discussed, consist of a bulk material known as the matrix and a reinforcing material or a filler material of some type, namely fibre, whiskers, particulate or films. The filler materials usually carry the major strength and loads while the matrix holds these together to enable the transfer of stresses and loads [8]. Identified by the matrix materials, composites are grouped into three broad groups, Plastics (Polymer Matrix Composites), Metals (Metal Matrix Composites) and Ceramics (Ceramic matrix composites). While we have discussed Polymer matrix composites at length in order to discuss the composites in general. Ceramic matrix composites

(cermets) are not within the scope of this thesis. Literature review has been conducted extensively on MMCs in general and Al-SiCp MMCs in particular.

Metal matrix Composites materials (MMCs) have been under development for about decades now. They were first developed for applications in aerospace, followed by application in other industries. [9]

In the MMCs there is a high degree of interaction between the matrix and the reinforcement which is reflected by the character of the interface developed between the two phases, pertaining to problems of chemical as well as mechanical compatibility of both of the constituents. Chemical compatibility has been addressed to in MMCs in two ways either using low temperature fabrication (solid-state) method or by selecting thermodynamically stable constituents that are at equilibrium with each other. A corresponding thermal- mechanical compatibility problem is addressed to by using a ductile matrix that yields & takes up all the differential strain in thermal alterations by selecting matrix and reinforcement having nearly matching thermal expansion coefficient.

Lloyd, D.J., [10], White house, et.al. [11] and Ribes, et al, [12] studied the effect of particle – induced damage in MMCs. They found out that with MMCs reinforced by particles with a size greater than 10 μ m, the dominant damage mechanism is cracking of particle and that the particle -matrix interface appeared to have little effect on the overall damage fracture behaviour. Thus the MMCs with particulates reinforcement do depend on the size of the particulates to a considerable extent. Song et.al. [13] and Qin, et.al. [14] inferred through extensive experimentations that the ductility and fracture

toughness of particle reinforced metal matrix composites (PRMMCs) are affected adversely due to the presence of the hard and brittle ceramic reinforcement. As a result of this, they claimed, many PRMMCs fractures with little warning that can be considered as detrimental to their structural applications. A detailed - analysis of failure - processes of PRMMCs was made by Lorca and Gonzalez [15]. They proposed that at the initial stages of plastic deformation the increase in load carried by the particles is mainly due to the progressive strain hardening of the surrounding matrix, which is relatively ductile. As the matrix strain hardening capacity is saturated relaxation of stresses from fractured particles result in the stress transfer to nearby particles causing greater particle fracture. They further inferred that the final fracture of the composites takes place by a ductile mechanism involving the nucleation and growth of voids in the matrix, which contributes to the final coalescence of the larger voids originating around broken particle.

In view of the above, Liu et. al [16] commented that matrix ductility is critical for the fracture toughness of PRMMCs. However, they observed that the mis-matches of the elastic modulus and coefficient of thermal expansion (CTE) between the matrix and the particulates reinforcement give rise to residual stresses in the matrix during the fabrication of the composite itself. In regions near the interface (matrix-reinforcement) large residual stress relaxations cause the strain hardening of the matrix. Again under load the applied stresses superimposed on residual stresses may cause further strain hardening of the matrix. Thus the strain hardening capacity of the matrix reaches its saturation point early, at a low value of the external strain levels only, which leads to the premature fracture of these composite. In addition, the compressive residual stresses at

the reinforcement- matrix -interface influence the decohesion of the interface and the behaviour of the interface to these stimulations is also responsible, along with other factors as discussed, for the fracture properties of these composites. Therefore, they suggested that it is essential to have a knowledge of the residual stress level and its distribution in the composites during fabrication, exposure to different ambient conditions, as well as when these are subjected to external load applications. The matrix and reinforcement will not be in thermodynamic equilibrium at the interface, i.e., there will be a driving force for chemical reactions between the two. Therefore, chemical compatibility between the two constituents of a MMC, must also be given due considerations while evaluating the composite. When one considers MMCs for ambient temperature applications, factors such as fiber / matrix adhesion must be considered. However, when service requirements demand short- term high temperature exposures thermo mechanical compatibility and resistance to the environment such as oxidizing ambient conditions will need to be addressed to. For long term high temperature applications, meaning exposure to thermally activated processes which may bring about inter diffusion and interfacial reactions between the matrix and the reinforcement, the challenges for characterizing the composite become much more critical.

Interdiffusion promoted phenomena in MMCs can have varied consequences on the integrity of a composite system. However, few of these effects like dissolution of the reinforcement, formation of intermediate phases at the interface, poisoning of the matrix by the fibre, poisoning of the fibre by the matrix and a general coarsening of the

reinforcement, may fail to have serious adverse effects on the composites properties; never the less these phenomena and their effect on composite properties must be understood, quantified and if possible, remedied before the advantages gained via a composite architecture can be fully utilized for long term, high temperature applications. Kopp, et. al. [17], while working with various MMC systems, have concluded that understanding inter diffusion between metal matrix composite components and its affect is essential in terms of material selection for long term, high temperature applications.

2.3 Al-SiC MMCs

In addition to having a metal or an alloy as the continuous matrix, the MMCs contain a reinforcement that can be particle, short fibre or whisker or continuous fibres. On the basis of the type of the reinforcement there are three kinds of MMCs; viz, particle reinforced MMCs, short fibre or whisker reinforced MMCs and continuous fibre or sheet reinforced MMCs. Of these three types, particle or discontinuously reinforced Macs have become very important because they are relatively inexpensive in comparison to continuous fiber reinforced composites and they have relatively isotropic properties compared to fibre reinforced composites.

Discontinuously reinforced (particle reinforced) Aluminum alloy based (DRA) metal matrix composites are viable candidates for use in weight-sensitive and stiffness-critical components [18-22]. The presence of the discontinuous reinforcement phase in

a continuous Aluminum alloy metal – matrix results in properties that are not attainable by other means. However, many researchers [23-26] have commented on limitations to the wide spread applications and use of these composites owing to their lower fracture toughness and poor tensile ductility compared to the un reinforced counter part.

Silicon carbide particulates (SiCp) are the most preferred reinforcements for aluminum alloy composites because of the enhanced achievable properties. For example, incorporation of the discontinuous particulate reinforcement in a ductile aluminum alloy metal matrix resulted in a 15-40% increase in strength and a 30-70% increase in stiffness, compared to the un- reinforced counterpart [27, 28]. The increase in strength is often more pronounced at elevated temperatures [29,30]. Improvements in elastic modulus of up to 100% have been reported for an aluminum alloy discontinuously reinforced with 40 % of silicon carbide by volume [31].

The mismatch in the co-efficient of thermal expansion between the SiC particle and the aluminum alloy metal matrix gives rise to a high density of dislocation both at and near the reinforcement / matrix interface. The enhanced expansion of the matrix induces plastic deformation during cooling with an associated increase in the density of dislocations [32]. One must appreciate that the DRA MMCs are amenable to conventional metallurgical processing, fabrication and characterization methods used for the un- reinforced aluminum alloy counterparts [33] and that this aspect of the composites may be considered as the single most advantage of the DRA MMCs.

The particle reinforced aluminum matrix composites (PRAMCs) have attractive material characteristics such as increased stiffness, wear resistance, specific strength &

vibration damping and decreased co-efficient in thermal expansion compared to conventional aluminum alloys. Also the fabrication of continuous fibre, short fibre and whisker reinforced aluminum matrix composite is associated with technical difficulties and is not cost friendly. Therefore, the PRAMCs have generated much interest in researchers resulting in every attempt at tailoring these groups of composites to suit various applications [34].

Looney, et.al. [35], after thorough investigations, have concluded that the size and size distribution of aluminum powder used for manufacturing the PRAMCs strongly affect the sintering response of green components and therefore, affect the material characteristics of the sintered components greatly. They also suggested that as the volume fraction of SiC drops, the interaction during pressing between the SiC powder and the Aluminum powder reduces. Therefore, they proposed that the SiC particles size must be reduced in order to increase the incidence of inter action between the matrix forming Aluminum powder and the reinforcement i.e. the SiC powder.

Srivastan, et.al [36] have discussed the tensile properties and fracture characteristics of Aluminum alloy 2009, discontinuously reinforced SiCp. They claim that the increased strength of the composite is due to the following factors.

- (i) Residual stresses generated due to the differences in the CTE of the matrix and the reinforcement.
- (ii) Constrained plastic flow and tri axiality in the ductile Al. alloy metal matrix due to the presence of dispersed particulate reinforcements.

They further claimed that in a microscopic scale the fracture comprised of cracking of the individual and clusters of the SiC particles present in the microstructure and that the final fracture of the composite resulted from crack propagation through the matrix between the clusters of reinforcing SiC particles. On the basis of the analysis as given above, they concluded that:

- (a) The presence of hard, brittle and elastically deforming SiC particles in the soft, ductile and plastically deforming Al alloy metal matrix caused fine microscopic cracks to initiate at low values of applied stress.
- (b) Fracture of the matrix between the clusters of reinforcing particles coupled with particle failure by cracking and decohesion at the matrix particle interface allows the microscopic cracks to grow rapidly and link resulting in microscopic failure that led to a low tensile ductility value.

Chawla, et. al. [37] made a detailed study of the mechanical behavior and microscopic characterization of SiC particle reinforced aluminum matrix composites fabricated both by sinter forging and extrusion. They observed the following.

- (i) Sinter-forged sample exhibited higher young's modulus and improved ultimate tensile strength compared to the extruded material.
- (ii) The extruded material exhibited higher strain to failure values while the higher values of young's modulus and UTS were attributed to the absence of any significant processing- induced particle fracture, the lower strain to failure was attributed to poorer bonding between the matrix and the reinforcing particles of the sinter forged test sample compared to the extruded one.

It has been established beyond doubt [38], when limited to a thin layer, chemical reactions between the matrix and the reinforcement promote intimate interfacial contact

there by raising the strength of the metal ceramic bond resulting in an improvement in the bulk mechanical properties of the composite. The interfacial reactions may take place either when the composite is being fabricated or when it is put to service. It is observed [39, 40] that SiC particles in Al/SiC composites may react with liquid Aluminum to form Aluminum carbide and silicon, during processing itself.

The dominant void nucleation modes in particle reinforced MMCs are brittle cracking of the reinforcing particles and decohesion along the particle- matrix interface. When the interfacial bond strength increases the tendency of formation of voids (cavitations levels) is decreased at the particle-matrix interface [40] and interfacial decohesion gives way to particle cracking [41,37]. The ductility may increase due to void - nucleation-taking place on account of particle cracking. This is because in case the interfacial bonding is well established; it acts as a greater constraining factor for matrix deformation in which case particle cracking can be considered to be the only factor for explaining the increase in ductility [42]. It must, however, be well understood that in a composite, the plastic flow of the matrix is constrained by the presence of the reinforcing particles and that with strongly bonded interface, the volume of the matrix deforming plastically is reduced which result in a decrease in the ductility.

In light of the above, Tham, et. al [43] made certain very important observations as given below.

- (i) The strain to failure in a composite is primarily governed by the volume fraction of the matrix phase that could flow plastically during deformation.

- (ii) Formation of a thin reaction layer along the interface changes the fracture pattern from one involving interfacial decohesion to one where particle cracking is dominant.
- (iii) High reinforcement concentration and /or thick reaction layers lead to very low strains to failure.

2.4 Processing of Metal Matrix Composites

Despite of the highly promising mechanical and thermal properties of MMCs for a long time these did not get the recognition for multipurpose use and rather had a limited use in very specific applications. The single most pronounced factor was the complex processing requirements and thus the high cost involvements that ultimately had a greater say on the price of the final composite articles. From this point of view improvements in the composite processing techniques have invited appropriate considerations for increasing the commercial applicability of the MMCs. Indeed, significant efforts have been and continue to be, devoted towards this end with encouraging results.

Processing of MMCs can be broadly divided into two categories of fabrication techniques. They are:

1. Solid state (powder metallurgy and diffusion bonding) and
2. Liquid state.

2.4.1 Liquid state processing of MMCs

The advantages of this process include the ease of handling liquid metals compared to their powder counter parts; lower cost involvements for obtaining liquid metals than metal powder; possibility of producing various shapes using liquid metals with considerable ease by adopting methods already developed in the casting industry for unreinforced metals etc. Conversely liquid state processing also suffers from a number of factors that include lack of reproducibility associated with incomplete control of the processing parameters and some undesirable chemical reactions at the interface of the liquid metal and the reinforcement[45A]. However, despite the difficulties associated with it, a majority of the commercially viable applications of MMCs recommend for liquid state processing.

Liquid state processing techniques utilize a variety of methods to physically combine the matrix and the reinforcement. On this basis, the liquid state processing can be grouped into four major categories. They are:

1. Infiltration
2. Dispersion
3. Spraying and
4. In-situ fabrication

2.4.1.1 Infiltration Processes

In this process a porous body of the reinforcing phase is held within a mold and is infiltrated with molten metal that flows through the interstices of the reinforcement to fill the pores, thereby forming the composites. The liquid metal generally does not wet the porous reinforcement phase spontaneously. Therefore, often it is forced into pre-form of reinforcement by the application of an external force. The external force applied overcomes the capillary and forces that might otherwise oppose the entry of the liquid metal into the porous pre-form. The variables involved in the infiltration process include the initial composition, morphology, volume fraction and temperature of the reinforcement; the initial composition and temperature of the infiltrating metal and the nature and magnitude of the external force applied to the metal, if any. [45A].

Major advantage of infiltration processes is that they can ensure near-net shape production of parts fully or selectively reinforced with a variety of materials. The process also ensures minimum matrix reinforcement chemical reactions and defect free matrix microstructure if cold dies and reinforcements are used or if pressure is maintained during solidifications. The limitation of the process however is the availability of the reinforcement that must be self-supporting as a bound pre-form or as a dense pack of particles or fibers. The tooling may be expensive if high pressures are needed. Heterogeneity of the composite may result if the pre-form deforms during infiltration or fibers get clustered during fabrication. These, if they happen, may affect the mechanical properties of the composite adversely.

On the basis of the nature and magnitude of the external force alone the infiltration process are grouped into several categories. They are as follows.

- (a) No External force
- (b) Vacuum – Driven Infiltration
- (c) Pressure – Driven infiltration and
- (d) Other forces

2.4.1.1.1 No External Force

In specific cases, however, metal may spontaneously infiltrate the reinforcement. Cermets such as titanium carbide reinforced steel or nickel base alloys have then produced by spontaneous infiltration [44]. In certain specific cases the system may have specifically tailored chemistry or processing conditions to induce wetting of the reinforcement by the liquid metal so that spontaneous infiltration is induced. An example in this category is provided by Harington, et. al. [45] concerning Ti – B process in which Ti and B are deposited by chemical vapour deposition on fibres prior to infiltration by Aluminium. Another example is the PRIMEX pressure- less metal infiltration process [46] developed by Lanxide corporation, NewYork. Here an Al-Mg alloy infiltrated ceramic pre-form at temperature between 750° C and 1050⁰ C in a nitrogen rich atmosphere. However, the reported rates of infiltration were quite low up to 25 cm / hour only.

2.4.1.1.2 Vacuum Driven Infiltration

In some systems creating a vacuum around the reinforcement provides a sufficiently large pressure difference to drive infiltration. One interesting technique of

vacuum infiltration involves the up ward infiltration of magnesium into encased pre-forms of Al_2O_3 or SiC . Either the molten metal or its vapour reacts with the air above the pre-form to form solid products such as MgO . The vacuum thus created provides the driving force for infiltration.

2.4.1.1.3 Pressure Driven Infiltration

This process involves mechanical work to force the metal into a pre-form that it does not wet. In addition to providing the pressure to overcome the capillary forces, the pressure driven processes also provide for advantages such as increased processing speed, control over chemical reactions, refined matrix microstructures, better soundness of the product through feeding of solidification shrinkages, etc. The pressure may be applied by a gas or by a mechanical means. Pressure application by gas involves forcing of the metal in to the pre-form of reinforcing phase by an inert and prescribed gas such as Argon. Mechanically applied pressure involves a force that is exerted on the molten metal by the piston of a hydraulic press. This pressure is maintained throughout the solidification process.

Composites processed by application of pressure generally have a pore free matrix. However, the application of pressure may induce pre-form deformation or even breakage during infiltration.

2.4.1.1.4 Other forces

Alumina pre-forms are infiltrated by Al-Si alloys under low pressure with the assistance of vibrations [47]. Centrifugal casting methods have then adopted for

producing a tubular reinforced metal [48]. Recently, a new infiltration process has recently been developed by using electro magnetic forces to drive molten metal into a pre-form [49].

2.4.1.2 Dispersion processes

In dispersion processes the reinforcement is incorporated in loose form in to the metal matrix [45A]. Since most of the metal reinforcement systems have poor wetting properties, a mechanical force is usually required to combine the phases in the way of stirring. This process is the most inexpensive process for production of MMCs, which can be further processed by casting or extrusion.

The simplest dispersion process in current use is the vortex method. In this method the liquid metal is vigorously stirred and the reinforcement particles are added in the vertex [50]. Skibo and Schuster [51] have patented a process for mixing SiC particulate in molten Aluminum under vacuum with a specially designed impeller. It is claimed that the process has the advantage of limiting the incorporation of impurities, oxides or gasses because of the vacuum and the reduced vertexes.

Another process involves a follow mixing where a rotating blade is progressively lowered in to an evacuated bed of particles covered with Molten aluminium. Yet another process involves injection of particles below the surface of the molten metal using a carrier gas.

The limitations of the dispersion processes lies in the poor control over the undesirable features such as porosity resulting from gas entrapment during mixing, oxide inclusions, reactions between matrix and the reinforcement in view of the long

contact times and particle migration and clustering during and after mixing. Also these processes are not suitable for long fibers or oriented reinforcements because of the difficulties in stirring and the need for adapting secondary deformation processing for improving reinforcement distribution and closing any pores.

2.4.1.3 Spray processes

In these processes droplets of molten metal are sprayed together with the reinforcing phase and collected on a substrate where metal solidification is completed. Also the reinforcement may be placed on the substrate and the molten metal may be sprayed on it [45A].

The critical parameters in these processes include initial temperature, size distribution and velocity of the metal drops; the velocity, temperature and feeding rate of the reinforcement. The position, nature and temperature of the substrate collecting the material are also important. Most spray deposition processes use gases to atomize the molten metal in to fine droplets. The reinforcing particles can be injected with in the droplet stream or between the liquid stream and the atomizing gas.

The spray deposition technique renders a fine microstructure of the matrix metal with fine grain size and low segregation. Also due to the smaller times of contact the interfacial reaction between the reinforcement and the matrix is minimized. This will result in a thermodynamically meta- stable two-phase material.

The drawback of the process is a higher amount of residual porosity (at least a few percent by volume). This factor leads to a further processing of the materials. This process of spray processing is not as economical as the dispersion or the infiltration

processes. This is because of the use of the costly gases and the resulting large amounts of waste powders that need to be collected and disposed.

2.4.1.4 In Situ Process

The term In-Situ composite was first used for materials produced by solidification of poly phase alloys. When the poly phase alloys solidify directionally with a plane front, they may show a fine lamellar or rod like structure of β phase in an α phase matrix, the inter phase spacing being a function of the growth rate. These materials have been suggested for use in the areas of optics and electronics. However, their low growth rates and problems resulting from the gradual coarsening of the structure at elevated temperature have restricted their use. Recently an effort has been made to produce reinforced inter-metallic alloys by controlled solidification, chemical reactions between a melt and a solid or gaseous phase, etc.

Another way to produces In-Situ composite is to react molten metal with a gas. Examples include the production of Al_2O_3 / Al composites by oxidations of Aluminum [52]. Injecting a gas like CH_4 or Argon through a melt like Al - Cu – Ti can be used to produce wide range of carbide and nitride reinforced alloys [53]

Advantage of this process includes a homogeneously distributed reinforcement [45A]. The spacing or size of the reinforcement can be controlled by adjusting the solidification or reaction time. However, the limitation include the choice of the system; orientation of the reinforcement, etc. Sometimes it may also be difficult to control the kinetics to control the reaction or the shape of the reinforcing phases.

2.4.2 Solid - State Processing of MMCs

Solid state processing of MMCs are generally used to obtain the highest mechanical properties in the resulting MMCs. Particularly the discontinuous reinforcement MMCs are processed in this route to obtain enhanced mechanical properties. This is because the solid-state processing methods keep the segregation effects and brittle reaction products formation, especially when compared with liquid state processes, at a minimum.

2.4.3 Primary solid-state processing of Discontinuously Reinforced Composites

Particulate reinforced composites are processed in a variety of techniques. These include the following:

- (i) Powder Blending and consolidation
- (ii) Mechanical Alloying
- (iii) Diffusion Bonding or Roll Bonding
- (iv) High-rate Consolidation and
- (v) Powder Coating followed by solid- state consolidation.

2.4.3.1 Powder Blending and Consolidation

In this process the matrix metal (alloy) powder is blended with the reinforcing ceramic particulates (fibres). A green compact is obtained by cold Isostatic pressing and the green compact is sintered in a controlled atmosphere either in the solid state (with or without some liquid present) or in the liquid state. Alternately the green compacts are

thoroughly out gassed and forged or extruded to obtain the composite under question. In some cases hot Isostatic pressing of the powder blend is carried out after complete out gassing.

Most powder consolidation and processing work is carried out below the matrix solidus temperature. However, sometimes it becomes necessary to maintain the consolidation temperature slightly above the solidus. This helps minimize the deformation stresses and avoids any particulate (whisker) damage during processing. In liquid state sintering, powder consolidation may be achieved without the use of any external pressure since a low melting phase pulls solid particles together due to the surface tension. In order to impart appropriate bonding and the creation of a well-defined interface the higher melting phase should be slightly soluble in lower melting matrix in consolidation processes carried out by liquid – state sintering.

2.4.3.2 Mechanical Alloying

Mechanical Alloying is truly a solid- state process that can be applied to particulate composites. In this method a high- energy impact is used to continuously fragment and reweld the powder particles as fresh internal surfaces are exposed. The continuous fragmentation leads to thorough mixing of the constituents and subsequent processes such as hot pressing, extrusion, etc., are used to consolidate the composite.

2.4.3.3 Diffusion Bonding or Roll Bonding

Diffusion Bonding is a solid- state creep deformation process. It is used for consolidating alternate layers of foils and fibres to create a simple ply or a multiply

composite. At the beginning creep flow of the matrix takes place in order to make complete metal-to-metal contact. After that diffusion across the foil interfaces completes the process. Pressure and time of pressure requirement for achieving appropriate consolidation can be determined from a knowledge of the flow stress of the matrix to actuate its flow between the fibres and across the foil interfaces. [45B].

Metallic foils and fibres / particulates can be subjected to roll bonding and co - extrusion to process the composite. This can be achieved in any of the two ways presented below.

Powder blends packed and evacuated in a container are subjected to the consolidation methods through roll bonding. Alternately, laminated composite are ideally produced by high temperature roll bonding operations starting from either foils of the alloy or of the individual metals. During roll bonding a strong interface is created by both, surface deformation and diffusion causing asperity deformation and inter diffusion.

2.4.3.4 High Rate Consolidation

This process of consolidation of powder blends is most suitable for rapidly solidifying (RS) and hard-to-deform metals.

Frictional heating at the metal powder reinforcing particle interface causes local heating and consolidation. The heat generated is rapidly extracted by the cooler-particles- interior that causes rapid solidification. Due to a remaining high dislocation density, high rate consolidation leads to strengthening of alloys. However the ductility is reduced. Composites produced by this method often contain cracks. In view of the

above, it is still desirable whether this method of MMC processing can really render reasonable composite properties.

2.4.3.5 Powder Coating followed by solid-state consolidation

The reinforcing powder is coated with a variety of metallic materials by electrochemical or vapour processes followed by solid-state consolidation methods. Composites made from coated particles have a reasonable amount of matrix spacing between the reinforcing particles. This can be considered as an advantage of MMC processing by coated particles because a chief cause of poor mechanical properties in composites originates from particle contact or too small an inter particle spacing. However coating methods adopted till date are not so advanced as to provide a contamination free uniform, thickness coating. On account of this seemingly disadvantageous reason few applications are using this method of composite processing. An example of this processing, however, includes hollow micro spheres of Al_2O_3 and quartz coated with a variety of metallic materials being consolidated into lightweight composites [54].

Blending and consolidation is the primary solid- state synthesis process used to produce both particles or whisker reinforced metal matrix composites. In this process pre-alloyed atomized powder of the matrix alloy (or elemental powder) is mixed with the powder or whisker of the ceramic phase (say SiC or Al_2O_3) and thoroughly blended. The matrix average particle size is 25 to 30 μm and the ceramic particle size needed to obtain reasonable mechanical properties is in the range of 1 to 5 μm . This large size difference creates agglomeration of the ceramic particles in the blend. Such agglomerations can be broken up during powder mixing by ultrasonic agitation in liquid

slurry. Also surfactants, which cause a repulsive force between the ceramic particles, can be used to improve the distribution of constituent phases. However addition of surfactants is usually avoided for metal matrix as this may cause contamination, which would adversely affect the mechanical properties of most of the MMCs. In view of this the most commonly used practice is dry blending in a v-blender or other agitation devices preferably carried but in an inert environment to avoid contamination.

Powder consolidation in MMCs is typically not a liquid-phase sintering process, though the liquid-phase sintering is adopted for some high temperature composite materials. Usually hot pressing or hot isostatic pressing is carried but at as high a temperature as possible to render the matrix in its softest solid-state condition. Generation of a liquid phase can adversely influence the mechanical properties of the products due to grain boundary separation and the formation of intermetallic phases. Most discontinuously reinforced MMCs are subjected to additional deformation processing to improve their microstructure and mechanical properties after full consolidation. These deformation processes also render a product of useful shape.

2.5 Deformation Processing of Metal-Matrix Composites.

Secondary deformation processing of the consolidated discontinuously reinforced composites leads to frame of particle / whisker agglomerations, reductions or elimination of porosity and improve particle-to-particle bonding. These factors separately or collectively tend to improve the mechanical properties of the MMCs.

These secondary deformation processing may include extrusion / rolling / forging of the MMCs.

2.5.1 Extrusion of Consolidated MMCs

The most common secondary processing of MMCs is extrusion. It is performed at a temperature, which ensures relatively high strain rate sensitivity. The process typically carried out at a high strain rate, primarily involves dislocation, creep deformation of the matrix. The highest possible strain rates are essential to obtain the most uniform flow of the matrix and to minimize tendencies of cracking of the reinforcing phase. Apart from improving the homogeneity of the product in extrusion can produce net-shape product forms in large lengths.

The presence of 15 to 25% non-deformable particulates (or whiskers) as in Al-SiC MMCs may cause fracture of the reinforcing phase during extension. To avoid this an appropriate process designing must be adopted. Gunashekhar, et. al [55], have shown that the use of streamlined dies can produce many complex section shapes without cracks which would be impossible to obtain with conventional extrusion die shapes.

2.5.2 Rolling of Consolidated MMCs

Extrusion is followed by rolling if sheet or plate products are desired. Edge cracking is a serious problem in rolled products compared to extrusion since rolling involves lower compressive stresses than extrusion. Therefore rolling to less than 40mm thick sections often leads to a significant amount of cracked material while has to

be ultimately scrapped. Rolling of discontinuously reinforced MMCs is most successful in the range of 0.5 T_m (melting temperature) using low roll speeds.

Warm, isothermal rolling using smaller passes and a large roll diameter produces sheets out of the discontinuously reinforced MMCs with a minimum of edge-cracking problems. However, when rolling at relatively lower temperatures reductions per pass must be minimized and intermediate-annealing steps must be utilized to obtain a defect free product.

2.5.3 Forging of consolidated MMCs

Automotive connecting rods, missile component, navigational systems, structures for space applications etc, are recently being fabricated as composite forged products. However, it must be noted that forging of these components from MMCs is often limited by cracking in the outer surface caused during the process of forging itself. It has been found that the work piece in a closed die forging operation may develop an incipient surface crack at an intermediate shape of forging. The surface crack, however, may no longer be visible at the end of the forging operation done to the pressing of the work piece against the die.

Closed up surface cracks are not acceptable for fatigue-loaded structures and so knowledge of forging limit [56] for the appearance of outer surface cracks is essential.

2.6 A Bird's Eye-view of The Literature surveyed

Table 1

(A) Characteristic properties and characterization of composites including Al-SiCp composites

Sl. No in the Bibliography	Name of Author/Authors	Conclusive findings
1.	Ashby, M.F.	New materials can be tailor –made with unique properties for specific end uses.
2.	Matthews, F.L., and Rowlings, R.D.,	Specific properties like no significant moisture absorption, non-inflammability high electrical and thermal conductivities of MMCs as compared to polymer matrix composites.
3.	Butter worth, Heinemann	Various applications of metal matrix composites.
4.	Alcan Aluminum corporation, Product Brochure	Enhancement of mechanical properties of reinforced metals with simultaneous degradation of ductility and fracture toughness.
5.	Ray, et.al	Enhanced applications of FRP composites over their metallic counterparts.
6.	Smith, F.W.	Matrix is the source of composite toughness
7.	Kalam, A.P.J.A and Tiwari, A	Specific use of FRP composites in aeronautics industries
8.	Jagnes, et.at.	The matrix in MMCs holds the reinforcing materials and is responsible for transfer of the stresses and load to the reinforcement.
9.	IBID, 3-1	MMCs are first developed for use in aerospace followed by applications in other industries.
10.	L loyd, D.J.	The dominant damage mechanism in MMCs

11. 12.	White house, et. Al. Ribes, et. Al.	reinforced with particles with a size greater than 10 μ m is cracking of the particle. The particle-matrix interface has little effect on the overall damage–fracture behaviour.
13. 14.	Song, et. Al. Qin, et. Al.	The presences of hard and brittle ceramic reinforcements adversely affect the ductility and fracture toughness of particle reinforced metal matrix composites.
15.	L lorea, et. Al.	Suggest the progressive strain hardening of the ductile matrix. They suggest that the final fracture of the composite takes place by a ductile mechanism involving mechanism and growth of voids in the matrix. Finally these voids lend to coalescence of larger originating around larger particles.
16.	Liu, et. Al.	Matrix ductility is critical for the fracture toughness of PRMMCs. Mismatch in the CTE of the matrix and the reinforcement gives rise of residual stresses in the matrix during fabrication of the composite itself.
17.	Kopp, et. Al.	Interdiffusion of the component of MMCs helps in selecting the components for composite processing for long-term high temperature applications.
18. 19. 20. 21. 22.	Srivastan, T.S. Kocjak, et. Al. Mc Gujre, P.F. Hunt, et. Al. L lyod, et. Al.	Discontinuously reinforced Aluminium Alloy composites find their use in weight-sensitive and stiffness critical component. The discontinuous reinforcement in Aluminium alloy metal matrix develops properties not attainable by other means.

23. 24. 25. 26.	Sugimura, et. Al. Liwa. et. Al. Davidson, D.L. Manoharan An, et. al.	The factors limiting the use of the DRA composites are the low value of fracture toughness and poor tensile ductility compared to the unreinforced alloy.
27. 28.	East, W.F. Demeis, R	They have quantified the increase in strength and stiffness of SiC particulate reinforced ductile Aluminium alloy. They remain that SiCp is the most preferred reinforcement for Aluminium alloys.
29. 30.	Nair, et. al. Mc Danels, D.L.	They conclude that the increase of strength of the SiCp reinforced Aluminium alloy Composites becomes more pronounced at elevated temperatures.
31.	Wills, T.C.	Established up to 100% improvement of elastic modulus by incorporation of 40% SiCp reinforcement in an aluminium alloy compared to the unreinforced alloy.
32.	Davis, et, al.	The mismatch in the CTE between the SiCp and Al. alloy matrix gives rise to a high density of dislocation at and near the matrix-reinforcement interface.
33.	Vogel, sand et. al.	DRA MMCs are amenable to conventional metallurgical processing.
34.	Sinclair, et.al	PRAMCs have attractive material characteristics fabrication of continuous fibre, short fibre or whisker reinforced Aluminium matrix composite is not cost friendly.
35.	Looney, et. al	SiC particle size must be reached in order to increase the incidence of interaction between

		the matrix forming Al powder and SiCp reinforcement.
36.	Srivastan, et. al.	Al-SiCp MMCs develop a higher strength because of the residual stress as a result of CTE mismatch and the considered plastic flow of the matrix Al. due to the triaxiality of the ductile Al. as a result of the presence of the dispersed reinforcement.
37.	Chawla, et. al.	Compared the mechanical behaviour and micro structural characteristics of both sinter-forged and extruded Al-SiCp composites sinter-forged ones show higher Young's modulus and U.T.S values. Extruded ones showed strain-to-failures.
38.	Tham, et. al.	When limited to a thin layer, chemical reactions between the matrix and the reinforcement promote intimate inter facial contact and therefore, the strength of the metal-ceramic bond.
39.	Iseui, et.al.	Sic particles may react with liquid Al. to form Aluminum carbide and Si, during processing itself.
40.	Warren, et. al.	
41.	Whitehouse, et.al.	With increase in the interfacial bond strength, the cavitations levels, i.e. formation of voids is decreased at the matrix particle interface.
42.	Mummery, et. al.	A strong interfacial bonding acts as a constraining factor for matrix deformation. In this case particle cracking can be considered as the only factor for increase in the ductility.
43.	Tham, et.al.	The strain to failure in a composite is primarily governed by the volume fraction of the matrix

		phase that flows physically during deformation.
44.	Lenel, et.al	Spontaneous infiltration of reinforcement can be a route for processing of composites.
(B).Processing of Composites		
45.	Harington, et.al	Specifically tailored chemistry or processing conditions can be created to induce wetting of the reinforcement by the liquid metal to encourage spontaneous infiltration.
46.	Kennedy, C. R.,	PRIMEX pressure less metal infiltration process developed by Lanxide Corporation, New York.
47.	Pennander, et. al.	Low pressure assisted by vibration can be utilized for processing of MMCs.
48.	Tsunekawa, et.al	They adopted the centrifugal casting route to produce reinforced metal matrix composite of tubular shape.
49.	Andrews, et.al	Electromagnetic forces can be used to drive liquid metal into perform to produce metal matrix composites.
50.	Rohatgi, et.al	They have stated about the processing of MMCs by dispersion processes in the vertex method. In this method liquid metal is vigorously stirred and the particles of the reinforcement are introduced at the vertex of stirred metal to cause dispersion.
51.	Skibo, et al.	The authors have patented a method of processing MMCs by dispersion methods in which they used a specially designed impeller to disperse SiCp in mol ten Aluminum.
52.	Xiao, et. al.	The Authors have mentioned about in-situ

		processes of production of MMCs. They have given the example of Al_2O_3 /Al composites by a process of oxidation of Aluminum.
53.	Sahoo, et.al.	CH_4 or Ar gas injection through a melt of Al-Cu-Ti can be used to produce wide range of Carbide and Nitride reinforced alloys.
54.	Rawal, et. al.	Hollow micro spheres of Al_2O_3 and Quartz coated with a variety of metallic materials are being consolidated to generate light-weight composites.
55.	Gunasekhar, et. Al.	They have reported about the design of an appropriate die for extrusion of the MMCs (Al-SiCp) and claim that the use of the specially designed die renders complex section parts without cracking of the reinforcement.
56.	Syu, et.al.	Knowledge of forging limit is a must while processing the MMCs which are to be exposed to fatigue loading, during forging of the MMCs.
57.	Sritharan, et. al.	Modification of surface chemistry of SiC by development of SiO_2 layer over it through heat treatment.
58	Witners, et. al.	Relaxation of residual stresses in Al/SiCp MMCs over long periods of time has been observed at room temperature.

2.7 Conclusions

The literature survey has been exhaustive. The work of several workers have been thoroughly studied and their conclusive findings have been recorded concerning the characteristic properties the characterization and the processing of composites through various routes. The initiation and mechanism of failure, the strain to failure, and the decrease of ductility and fracture toughness associated with the increase in the strength properties of the MMCs in general and Al-SiCp MMCs in particular have been thoroughly analyzed on the basis of the work conducted by various workers. Also the various methods of processing MMCs, their advantages and limitations have been discussed while trying to bring about a comparison between the MMCs processed through various routes. At the end of the chapter the conclusive findings of the investigators have been presented in a tabular form.

CHAPTER 3

EXPERIMENTAL

3.1. Introduction

This chapter describes the experimental procedure as adopted in the present project-work. The Equipment/Instruments utilized to carry out the experiments are listed in a tabular form indicating their specific use in the project along with their specifications and particulars in details.

A detailed report is also provided on the raw materials used for fabrication of the MMC test specimens and the characterization of the raw material used for fabrication. The chapter houses a description of the detailed step-wise methods adopted for fabrication of the test specimens, the thermal treatment imparted, the Mechanical testing carried out and generation of the micrographs through Scanning Electron Microscopy for their detailed analysis.

The photographs of the Equipment/Instruments used in the present work are also presented.

3.2. Equipment / Instruments Used

Table No.2 presents a detailed list of the Equipment/Instruments used in the present investigations along with their specific use in the experiments conducted and their detailed specifications.

3.3 Equipment / Instruments used In the Present Investigation

TABLE-2

Sl.No.	EQUIPMENT / INSTRUMENT	SPECIFICATIONS	USE IN THE PRESENT INVESTIGATION
1.	Particle size Analyser	Model-Micro P Make – Malvern Range – 0.05 - 550 μ	For ascertaining the particle size range of Aluminium powder as well as SiC particulates.
2.	Planetary Ball Mill	Model-PULVERISETTE-5 Make-FRITSCH, Germany Medium-Zirconia balls of different sizes (10mm 25mm, 50mm) Container –Zirconia bowls. Maxm speed of rotation-360 (RPM).	For mixing of the Aluminium powder and Silicon Carbide particulates thoroughly so as to obtain an uniform mixture, i.e. uniform dispersion of the SiC particulate re-enforcement in the Aluminium metal-matrix.
3.	X-Ray Diffractometer	Make-Philips Model-Analytical X-Ray X'Pert-MPD System Type-PW3040 2 θ range - 0 $^{\circ}$ -160 $^{\circ}$	For characterization of the individual raw-materials before mixing. For ensuring no pick up of Zirconia in the raw mix after mixing.
4.	Image-Analyzer	Model-Quantimet 570 $^{\circ}$ C Make-Leica	For deciding the optimum time of mixing at the specific speed of rotation adopted for ensuring an uniform dispersion of the SiC-particulate re-enforcement in the Aluminium powder matrix
5.	Cold-Universal Hydraulic Press	Make-SOILLAB Type-Hydraulic Max-Load-20 Tones	For preparing the green-shape of the test specimens by compaction which is to be subjected to Cold- Isostatic-press for further compaction.

6.	Cold-Isostatic Press	Make-STANSTED FLUID POWER Ltd., Type-Hydraulic Maximum Working Pressure: - 3000 PSI Product Canister: Inner Diameter- Ø97mm usable (max ^m) Inner Length 300 mm usable (max ^m)	Used for Cold-Isostatic pressing of the green pellets (Test Samples) as obtained after Cold-Uniaxial pressing.
7.	High Temperature Horizontal Tubular Furnace	Make - Naskar & Co. Type – Vacuum and Control Atmosphere Max ^m –Temp:-1750 ⁰ C Dim ⁿ s:- O.D–85mm I.D.–75mm Length – 500mm	Used for sintering the samples obtained after Cold-Isostatic pressing under N ₂ atmosphere at different sintering temperatures with different lengths of holding time.
8.	Drilling M/c.	Make - Royal Drilling High Speed Machine Model-Grade - I Machine No – 522	For drilling the sintered samples to obtain the ring-shaped samples to be subjected to compression test for obtaining the radial crushing strength.
9.	Electric Oven	Range- 30 ⁰ C to 300 ⁰ C	For exposing the samples to a thermal shock at + 80 ⁰ C, an elevated temp.
10.	Cryogenic Chamber	Make – S.D. Scientific Industries Ultra Low Chamber Range: +50 ⁰ C to – 80 ⁰ C	For exposing the samples to a thermal shock at – 80 ⁰ C, sub ambient temperature.
11.	Instron-1195	Make-Instron Ltd. Model-1195 Range-0.1N to 100KN	For Mechanical testing i.e. for carrying out the ring-test for obtaining the Radial Crushing Strength

12.	Scanning Electron Microscope (SEM)	Make-JEOL Type-JSM-6480LV	For obtaining the micrographs of the broken surfaces of the test samples which are already subjected to the ring-test.
-----	------------------------------------	------------------------------	--

3.4. Selection And Characterisation of Raw Materials

Research grade Aluminium metal powder and SiC particulates were obtained from the market. The assay of the materials as provided by the suppliers is provided below. These particles are analyzed for noting the size of the particles using the particle size analyzer. The data as obtained from the analysis is also presented below.

3.4.1. Aluminium Metal Powder

Assay 99.5% min
 Arsenic 0.0005% max
 Lead 0.03% max
 Iron 0.5% max
 Particle size 26.18µm

3.4.2. SiC Particulates

Alfa Aesar (A Johnson Mat they Company)
 Silicon Carbide 99% (Metal Basis)
 Particle size 33.62 µm

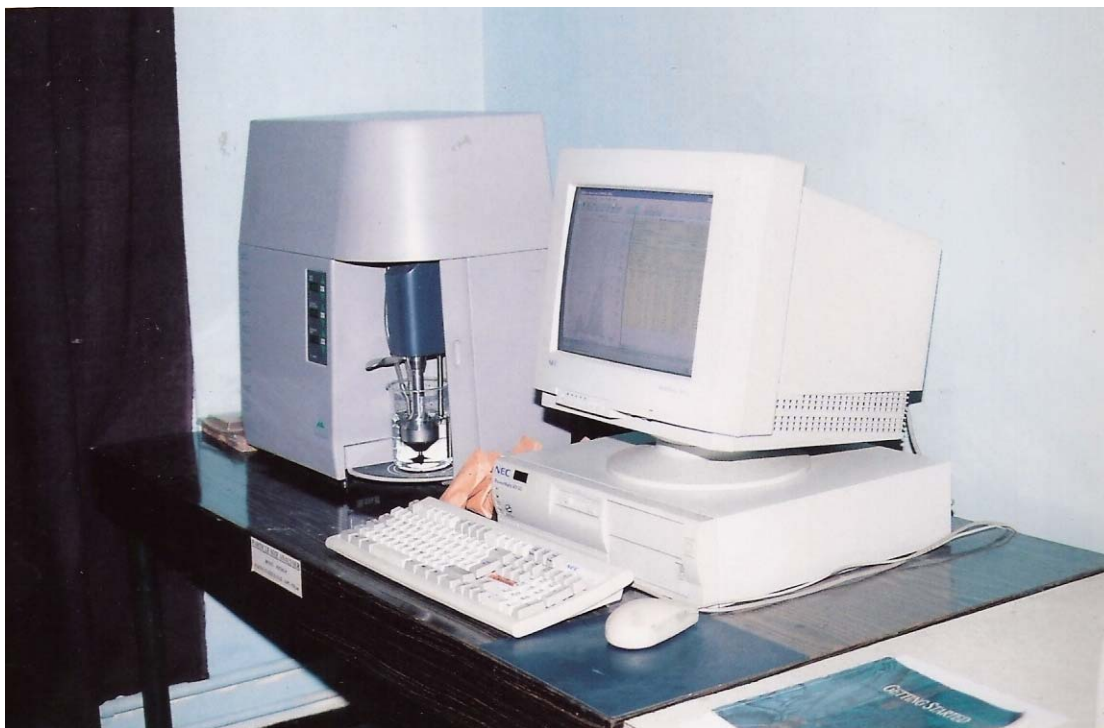


Fig. No. 1 – Particle Size Analyzer



Fig. No. 2 – Planetary Ball Mill



Fig. No. 3 – X – Ray Diffractometer



Fig. No. 4 – Image Analyzer



Fig. No. 5 – Cold Uniaxial Hydraulic Press



Fig. No. 6 – Cold Isostatic Press



Fig. No. 7 – High Temperature Tubular Furnace



Fig. No. 8 – Drilling Machine



Fig. No. 9 – Electric Oven



Fig. No. 10 – Cryogenic Chamber



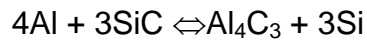
Fig. No. 11 – Instron 1195



Fig. No. 12 – Scanning Electron Microscope

3.4.3. Pre-treatment of SiC particulates

As prescribed by T.Sritharan et al [57], the SiC_p is heated to a temperature of 700⁰C in a muffle furnace in the presence of air and kept at the temperature for 60 minutes prior to using it for fabrication of the MMC samples. This is done in order to form a thin layer of SiO₂ on the SiC_p surface to make it inert to Aluminium so that the direct reaction between Aluminium and SiC_p is avoided which would otherwise produce Aluminium Carbide and Silicon following the reaction given below.



3.5. Fabrication of the Green Test Specimen

The Metal- Matrix- Composite test specimens are fabricated by the powder metallurgy route adopting the usual mixing and solid state sintering.

3.5.1. Mixing of the powders

75% Aluminium powder and 25% SiC particulates by weight are used for fabricating the composite specimens. The mixing is carried out in the planetary ball-mill in a zirconia medium. Zirconia bowls (2nos) and zirconia balls (25mm) are used. The speed of rotation is maintained at 250 rpm.

3.5.1.1. Optimisation of mixing time

The mixing is carried out for a period of 20 minutes and the m/c is stopped for 5 minutes. Then again the mixing is carried out for 20 minutes. In this way a total period of actual running of the machine is kept at 2,4,6 and 8 hrs. For each of the total time of running sampling is done to record the dispersion of SiC_p in the Aluminium matrix using

the Image- analyzer. The photographs obtained are presented in figure no.13. through figure no.16.

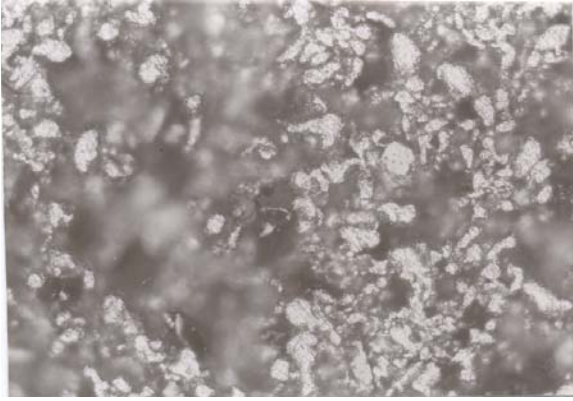


Fig no- 13 (2 hrs of mixing)

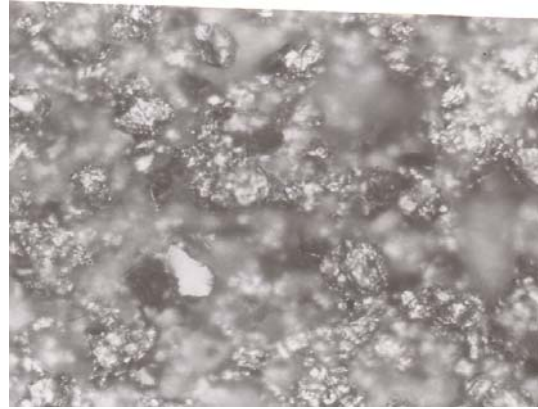


Fig no- 14 (4 hrs of mixing)

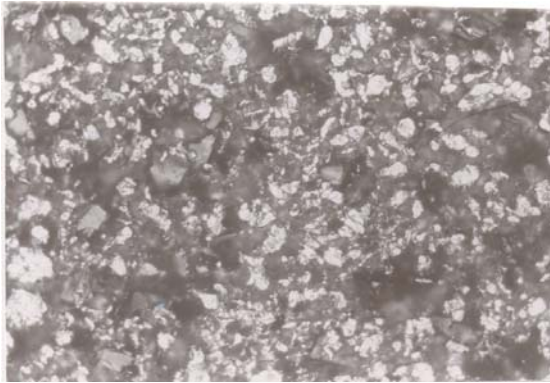


Fig no- 15 (6 hrs of mixing)

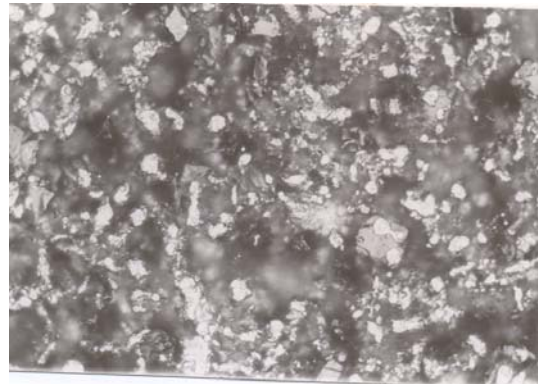


Fig no- 16 (8 hrs of mixing)

It is noticed that 6 hrs mixing time presented a uniform dispersion of SiCp; in Aluminium metal matrix, mixing time below 6 hrs. showed non-uniform dispersion, while at 8 hrs. mixing the SiC_p again got segregated as evident from the related photographs.

Thus the mixing time is optimized and is kept at 6 hrs. for 250 rpm speed of the planetary ball mill.

3.5.2. Compaction of the powder mixing

About 10 gms. of the powder mix is taken adopting a method of coning and quartering for compaction in a cold uniaxial press in a metallic die of inner diameter of 25mm.

3.5.2.1. Cold Uniaxial Pressing

The powder sample is pressed in the Cold uniaxial pressing machine, to render the green circular test samples of 25mm outer dia meter, applying a pressure of 4 tonnes psi.

3.5.2.2. Cold Isostatic Pressing

The green test picks are now subjected to Cold-isostatic pressing. For this purpose the green sample are kept in a rubber tube. The tube is evacuated and put in the oil bath in the cold-isostatic press and a pressure of 250 Mpa. is applied for compaction of the sample in cold state under isostatic pressure conditions.

3.5.3. Sintering of the Green Pellets

The green pellets of given dimensions obtained after Cold Isostatic pressing are subjected to sintering in the high temperature tubular furnace. Solid state sintering is adopted. Sintering temperature and the time of holding at a given sintering temperature are varied. The sintering temperatures adopted are 600⁰C, 580⁰C, 560⁰C and 540⁰C respectively. The holding time is varied as 2 hrs, 1.5 hrs and 1 hr, i.e., at each of the sintering temperatures different batches of samples are held for different lengths of time. A detailed nomenclature of the test samples is prepared as given below:

To start with, a batch of samples is placed in the tubular furnace, the tube is evacuated to a vacuum of 10^{-3} m bar and N₂ gas is passed through the tubular furnace

for the entire period of sintering to restrict the oxidation of the test specimen during sintering and holding the samples at the sintering temperature. Photograph of the sintered specimen is provided in Fig no.5

3.5.3.1. Nomenclature of the Test Specimens

A detailed nomenclature of the specimen is provided below in order to note and record the process variables to which the samples are exposed.

<u>Sintering Temp (°c)</u>	<u>Sintering Time (hr)</u>	<u>Designation</u>
a) 600	1	B ₁ T ₁
	1 ½	B ₁ T _{1 ½}
	2	B ₁ T ₂
b) 580	1	B ₂ T ₁
	1 ½	B ₂ T _{1 ½}
	2	B ₂ T ₂
c) 560	1	B ₃ T ₁
	1 ½	B ₃ T _{1 ½}
	2	B ₃ T ₂
c) 540	1	B ₄ T ₁
	1 ½	B ₄ T _{1 ½}
	2	B ₄ T ₂

3.5.4. Drilling of the Sintered Test Pieces

The determination of radial crushing strength by a compression test needs ring shaped samples. The circular sintered samples are now subjected to drilling to generate a ring shaped sample. A 6mm drill bit is used to perform drilling. Through out the process of drilling care is taken to see that the temperature of the sample is retained at the room temperature. To accomplish this the sample is drilled under a continuous spray of kerosene for the entire period of drilling. The sample before and after drilling is presented in Fig. no.17 & Fig no.18 respectively.

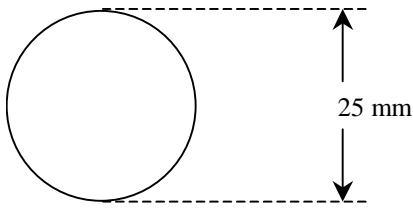


Fig no.17 : A sintered Specimen

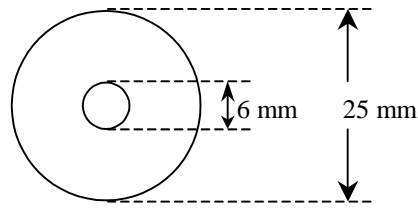


Fig no.18 : A drilled Specimen

3.6. Exposure of the Test Specimen to Thermal Shock

The samples are now exposed to thermal shock. For this purpose the samples, as per the nomenclature, are divided into two groups. One of the groups of the samples is kept at $+80^{\circ}\text{C}$ in the Electric Oven for a period of 1 hr. after the oven attained a temperature of $+80^{\circ}\text{C}$. Other group is placed in the Cryogenic chamber at -80°C for a period of 1 hr. After the chamber attained a temperature of -80°C , the groups of samples are separately collected in thermally insulated flasks and carried to the Instron Machine to carry out the testing for determining the Radial Crushing Strength.

3.7. Determination of Radial Crushing Strength

The radial crushing strength is obtained by testing the samples under compression using Instron-1195. A schematic diagram of the test process showing the holding of the test specimen is presented in Fig. No.19[37A].

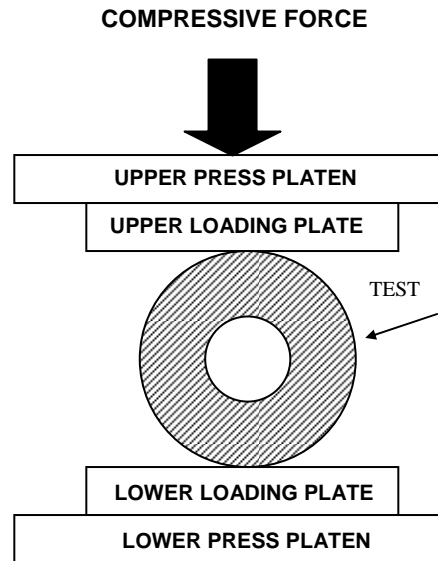


Fig. No.19 Experimental arrangement showing the holding of the ring shaped specimen.

The Radial Crushing Strength is obtained using the formula given below.

$$K = \frac{P \left(\frac{D+d}{2} \right)}{L \left(\frac{D-d}{2} \right)^2} = \frac{P(D-t)}{Lt^2}$$

Where:

K = radial crushing strength (MPa)

P=Breaking load (N)

D= Outside Diameter (mm)

d = Inside diameter (mm)

L = length (mm)

T = wall thickness (D-d)/2 (mm)

The test is a destructive test. The photographs of a specimen before drilling and a fractured specimen after the compression test are presented in Fig. No. 20 and Fig. No. 21 respectively.

3.8. Scanning Electron Microscopy

The broken test pieces are extensively examined in the Scanning Electron Microscope. This examination reveals the mode of failure undergone by the test samples, such as, the failure of the matrix; failure across the reinforcement; failure along the interface, etc.

3.9. CONCLUSION

This chapter, thus, provides an insight to the details of Experimental Processes and procedures as adopted in the present project work.

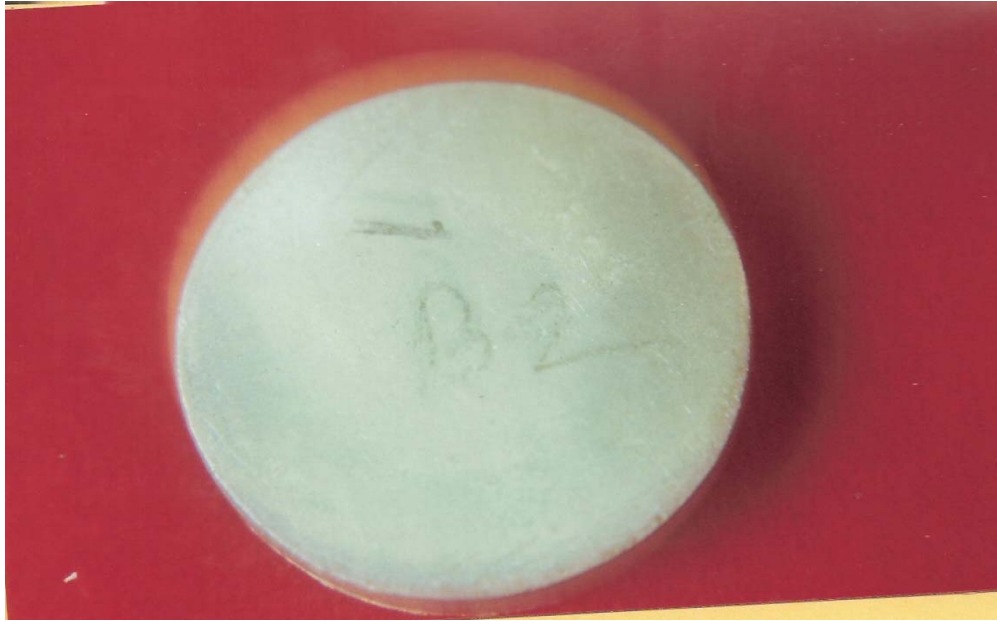


Fig. No. 20 – A Sintered Specimen before drilling

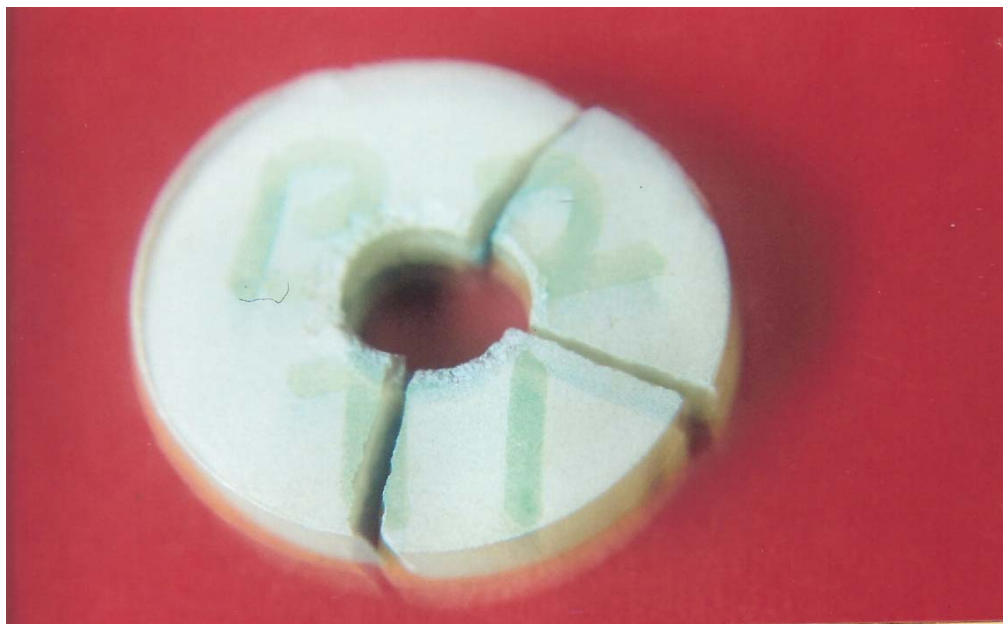


Fig. No. 21 – A Fractured Specimen after the compression test

CHAPTER 4
RESULTS
AND
DISCUSSIONS

4.1 Introduction

In this chapter the experimental findings are tabulated. Bar charts and the graphs are presented to record the variation of experimental data as a function of the experimental variables. The variations are explained with the help of the work of previous investigators and their findings. Also data are thoroughly analyzed on the basis of the SEM micrographs obtained.

4.2. Assessment and Evaluation of Mechanical Testing

4.2.1 Load at rupture under thermal shock

Table - 3
(The load values at rupture)

SI No	Sintering Temperature (°C)	Sintering Time (hr)	Load at Rupture (KN)	
			+80°C	-80°C
1	600	1.0	1.8880	1.3730
2		1.5	X	0.3730
3		2.0	1.0740	1.0020
4	580	1.0	1.0740	1.0230
5		1.5	X	X
6		2.0	X	X
7	560	1.0	1.3500	1.0630
8		1.5	0.8985	0.8771
9		2.0	0.6478	X
10	540	1.0	X	1.4390
11		1.5	1.2240	0.9974
12		2.0	1.4000	0.8020

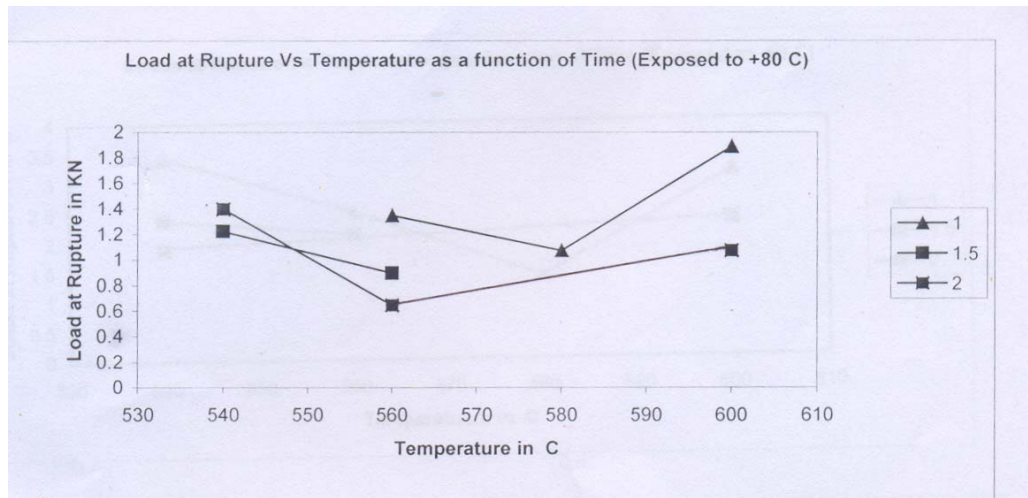


Fig No 22 - Load at rupture Vs Temperature as a function of Time (Exposed to +80°C)

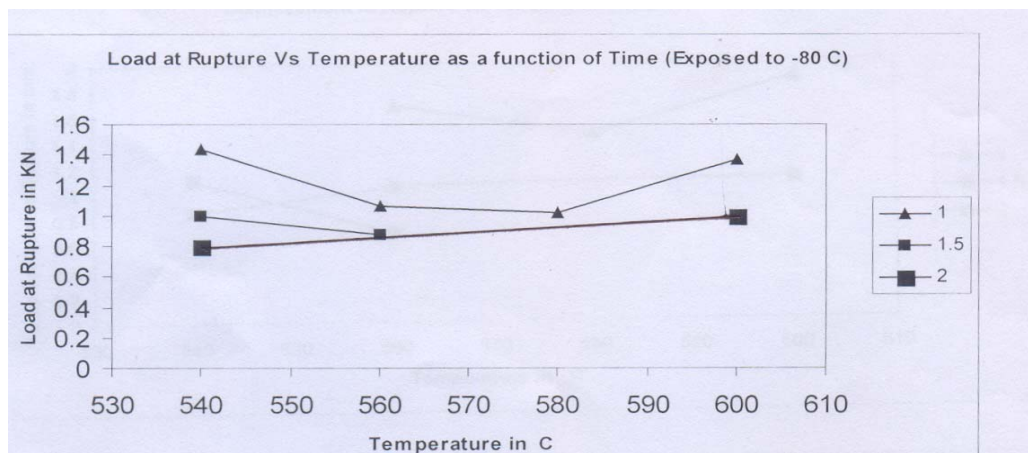


Fig No.23 - Load at rupture Vs Temperature as a function of Time (Exposed to -80°C)

Fig no.22 and Fig no.23 show the variation of the load at rupture for the samples held at different sintering temperature for different length of time and treated at $+80^{\circ}\text{C}$ and -80°C respectively.

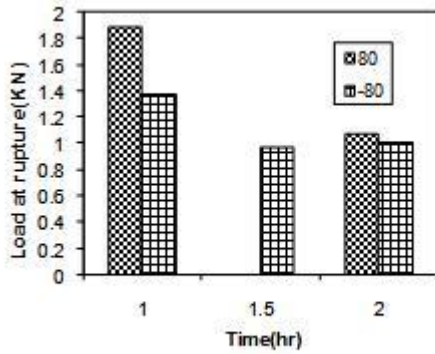


Fig no 24 : Bar diagram showing load at rupture V/s time at sintering temperature (600°C) for Samples exposed to $+80^{\circ}\text{C}$ & -80°C .

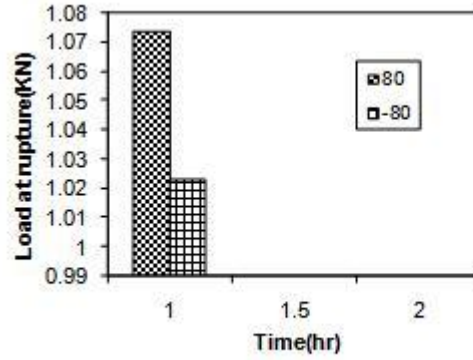


Fig no 25 : Bar diagram showing load at rupture V/s time at sintering temperature (580°C) for Samples exposed to $+80^{\circ}\text{C}$ & -80°C .

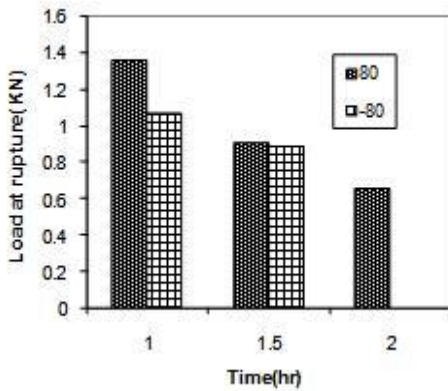


Fig no 26 : Bar diagram showing load at rupture V/s time at sintering temperature (560°C) for Samples exposed to $+80^{\circ}\text{C}$ & -80°C .

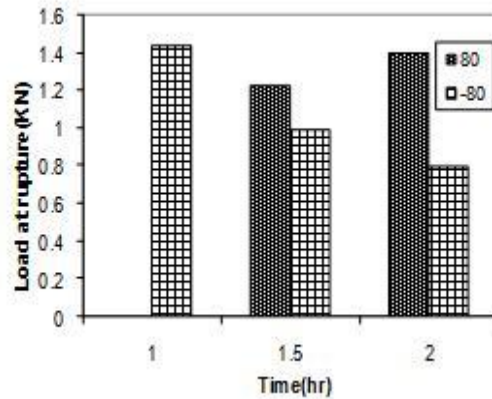


Fig no 27 : Bar diagram showing load at rupture V/s time at sintering temperature (540°C) for Samples exposed to $+80^{\circ}\text{C}$ & -80°C .

Fig no.24 through fig no.27 represent the bar diagrams for load at rupture as function of holding time at sintering temperature for samples treated at $+80^{\circ}\text{C}$ and -80°C respectively. The sintering times being 1, 1.5, 2hrs and the temperature being 600°C , 580°C , 560°C , 540°C .

Thermal shock due to treatment of test samples at $+80^{\circ}\text{C}$ and -80°C are less damaging for those samples, which are sintered at higher temperatures but held at the sintering temperature for shorter lengths of time. This trend is reversed for the samples, which are sintered at higher temperatures and held at the sintering temperature for longer length of time. This is evident from the fact that samples treated at 600°C and held at sintering temperature 1hr exhibit a higher value of load at rupture compared to the samples sintered at 600°C and held at the sintering time for 2hrs, when thermal shock is caused due to treatment at $+80^{\circ}\text{C}$. This trend is retained when thermal shock is caused due to treatment at $+80^{\circ}\text{C}$. However, the relative load value at rupture for samples treated at -80°C are lower than those for samples treated at $+80^{\circ}\text{C}$. The samples sintered at 580°C and held at sintering time for 1hr exhibits a higher value of load at rupture, when treated at $+80^{\circ}\text{C}$ than that when treated at -80°C . The samples sintered at 560°C also exhibit the same trend with load at rupture values when treated at $+80^{\circ}\text{C}$ being comparatively higher than those when treated at -80°C , but in both the cases the load at rupture values are lower than the respective values for samples sintered at 600°C .

Samples sintered at lower temperatures, away from the melting point of the Al. matrix show a increased resistance to thermal shock at $+80^{\circ}\text{C}$ with the increase in the holding time at the sintering temperature. This is evident from the fact that the load at rupture values are increased for the samples sintered at 540°C when the holding time at temperature is increased from 1.5hrs to 2.0hrs, with thermal shock being caused due to treatment at $+80^{\circ}\text{C}$.

However, when the thermal shock being caused due to treatment at -80°C this trend is reversed i.e. samples sintered at lower temperature (540°C) show an increase in the load at rupture values with the decrease in the time of holding at the sintering temperature. In all these cases, however, the highest load at rupture values when sintered at 540°C is lower than those at higher temperatures.

Sintering of the particulate reinforced metal matrix composites in the solid-state is accompanied by interatomic diffusion between the matrix and the reinforcement. This diffusion is temperature as well as time-at-temperature dependent and is responsible for the strength of the Al-SiCp composites becomes more pronounced at elevated temperatures [29,30]. This explains the relatively higher values of load at rupture as recorded experimentally at relatively higher temperatures and vice-versa.

However, with increase of the time of contact of diffusion increases resulting in a rigid interface. We know that when exposed to different environmental temperatures (such as $+80^{\circ}\text{C}$ and -80°C in this case) the composite experiences thermal shock. Also there is substantial difference in the thermal expansivity values between the Al matrix and the SiC reinforcement which gives rise to the generation of residual stress [16]. The relaxation of these residual stresses is limited by the extent of such diffusion, lower being the possibility of relaxation of the residual stress.

With increase in both the sintering temperature and the time at sintering temperature, the extent of inter-atomic diffusion increase which limits the relaxation of the residual stress. As a consequence of this there is substantial increase in the residual stress concentration, which result in lower values of the load at rupture, when the specimen is exposed to thermal shock. This explains the increased values of load at

rupture with the increase in the sintering temperature coupled with the decrease in the time for which the specimen is held at the sintering temperature. This trend is reversed, i.e. the load at rupture is decreased when the sintering temperatures as well as the time at temperature both are increased, due to higher extent of inter-atomic diffusion and lesser extent residual stress relaxation.

Samples sintered at a relatively lower temperature (say 540°C) respond differently to thermal shock as presented earlier, in this case, when the rupture values increase with at $+80^{\circ}\text{C}$, the load at rupture values increase with the increase of the duration of holding at the sintering temperature. However, when the thermal shock is delivered at -80°C the load at rupture values increase with the shortening of the time of holding at the sintering temperature as well as evident from data presented in table no.3 and plots at figure no.22

This phenomenon can easily explain considering that at lower temperatures due to lesser degree of inter-atomic bonding, the interface is relatively weak. The strength of the interface increases as the holding time at the sintering temperature increases due to greater extent of inter-atomic diffusion. Now when the thermal shock is due to treatment at $+80^{\circ}\text{C}$ there is enhancement of the interfacial bonding due to the fact that both the matrix and the reinforcement expand at $+80^{\circ}\text{C}$, with the matrix expanding at higher rate (about 7 times high) than the SiCp reinforcement. This enhancement is comparatively more pronounced for samples held at the sintering temperature for longer periods. In this way, at sintering temperature of 540°C and thermal shock at $+80^{\circ}\text{C}$, the samples held at the sintering temperature for longer periods of time exhibit a higher extent of resistance to rupture a physico-mechanical process.

For samples sintered at a lower temperature i.e. at 540°C , and exposed to thermal shock at -80°C , the resistance to rupture decreases with the increase in the holding time at the sintering temperature. This is because here a reverse physico-mechanical process, due to differential contraction between the matrix and the reinforcement having different thermal expansivities taking place. The one with longer holding time and relatively stronger interface with greater extent of inter-atomic diffusion, developing higher extents of thermally degraded area at or near the interface [32], due to this differential contraction as a consequence of limited relaxations in the resulting thermal residual stresses.

Fig no.24 through fig no.27 represents the same fact through bar-diagrams showing the loaded at rupture as a function of the holding time subjected to thermal shock at $+80^{\circ}\text{C}$ and -80°C respectively. To sum up:

At relatively higher temperatures the thermal shock is more damaging for samples held at sintering temperature for longer periods

The reverse happens when the time of holding at sintering temperature is shortened at relatively higher temperature of sintering.

The thermal shock at sub-ambient temperature is more damaging than at elevated temperature.

At relatively lower temperatures the resistance to rupture increases with time of holding at sintering temperature when the thermal shock is due to exposure to a temperature above the ambient temperature

The reverse takes place, i.e. the resistance to rupture is increased with the decrease of the holding time at relatively lower sintering temperatures when the thermal shock is due to an exposure to sub-ambient temperature.

The reason in general may be attributed, as discussed earlier, to (a) atomic migration or inter-atomic diffusion, (b) high residual stress due to limited or no release of the thermal residual stresses, when the interfacial bond is enhanced resulting in a strong interface, (c) Physico-mechanical processes at weaker interfaces due to misfit strain either due to compressive residual stresses as a result of differential expansion at an elevated temperature or tensile residual stresses as a result of differential contraction at a sub-ambient temperature between the Al matrix and the SiCp reinforcement.

4.2.2 Stresses at rupture under thermal shock

Table - 4
(The stress values at rupture)

Sl No	Sintering Temperature (°C)	Sintering Time (hr)	Stress at Rupture (MPa)	
			+80°C	-80°C
1	600	1.0	4.188	3.145
2		1.5	X	2.300
3		2.0	2.567	3.347
4	580	1.0	2.549	2.398
5		1.5	X	X
6		2.0	X	X
7	560	1.0	3.204	2.496
8		1.5	2.125	2.126
9		2.0	1.587	X
10	540	1.0	X	3.438
11		1.5	2.921	2.380
12		2.0	3.300	1.887

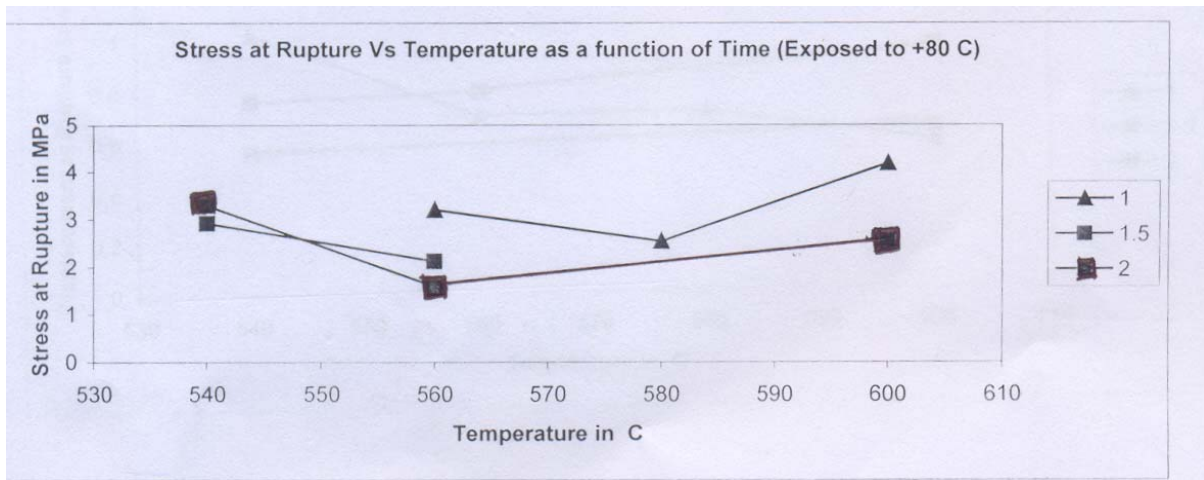


Fig No.28 - Stress at rupture Vs Temperature as a function of Time (Exposed to +80°C)

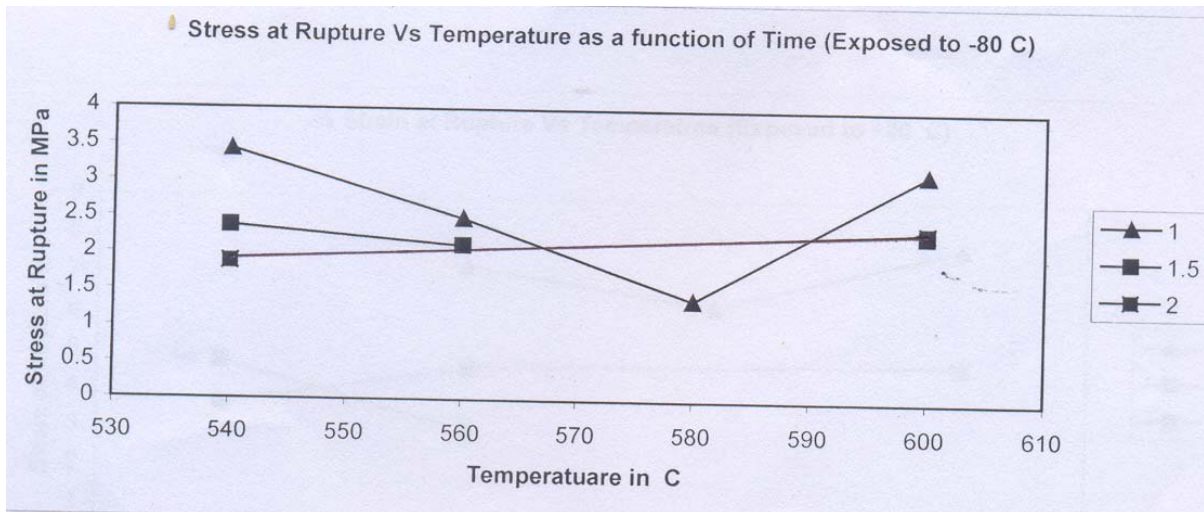


Fig No. 29 - Stress at rupture Vs Temperature as a function of Time (Exposed to -80°C)

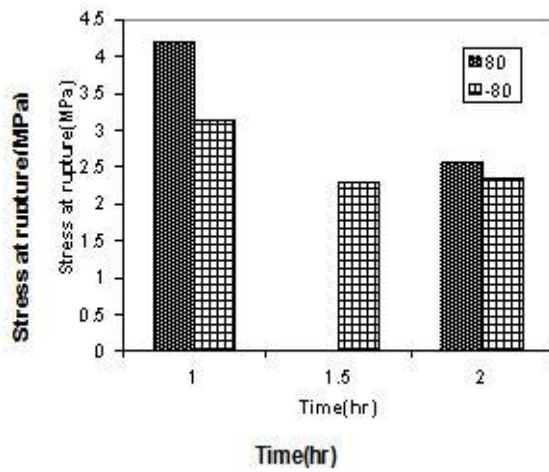


Fig no 30 : Bar diagram showing stress at rupture V/s time at sintering temperature (600°C) for Samples exposed to +80°C & -80°C.

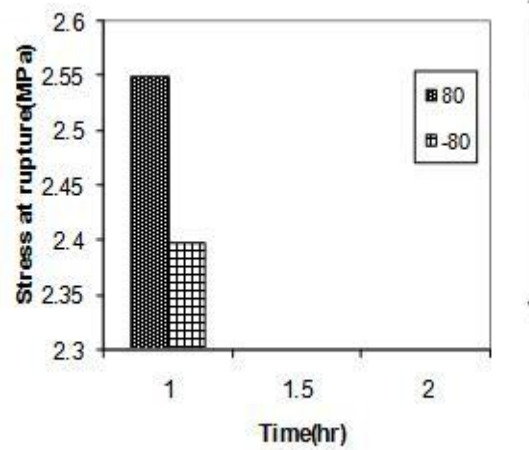


Fig no 31 : Bar diagram showing stress at rupture V/s time at sintering temperature (580°C) for Samples exposed to +80°C & -80°C.

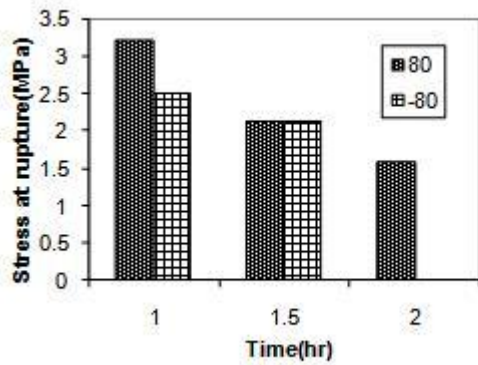


Fig no 32 : Bar diagram showing stress at rupture V/s time at sintering temperature (560°C) for Samples exposed to +80°C & -80°C.

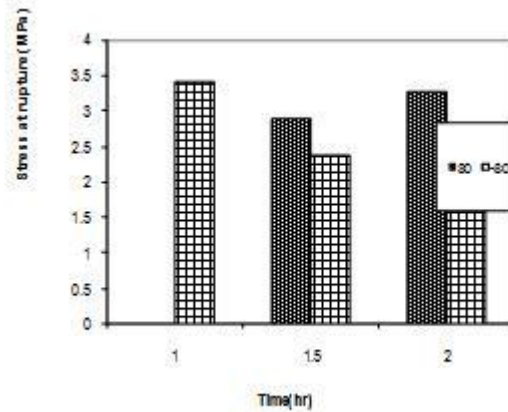


Fig no 33 : Bar diagram showing stress at rupture V/s time at sintering temperature (540°C) for Samples exposed to +80°C & -80°C.

These are plotted against temperature for various lengths of holding time at the sintering temperature and exposure to $+80^{\circ}\text{C}$ and -80°C as presented in the fig no.28 and fig no.29. Fig no.30 through fig no.33 represent the stress values at rupture at different sintering temperature as a function of the holding time at the sintering temperature when the samples are exposed to thermal shock at $+80^{\circ}\text{C}$ and -80°C .

Stress is defined as the load unit of the area exposed to the load. Needless to say that the trends of variation of stress at rupture follow a similar pattern as the load at rupture.

It is interesting to note the following from the experimental findings:

At relatively higher sintering temperatures and for short-term use (i.e. when specimen is exposed to the sintering temperature for short time) thermal shock is not much damaging.

However, thermal shock for samples with longer exposures, i.e. when exposed to long-term use seems to be more damaging, when relatively higher sintering temperatures are employed.

At relatively lower sintering temperatures the MMC responds well while put to long-term use even when exposed to thermal shock at an elevated temperature.

For short term use the thermal shock at an elevated temperature is more damaging for samples sintered at relatively lower temperatures.

For long-term use the thermal shock due to a sub-ambient temperature is more damaging when test specimen is sintered at relatively lower temperature.

Displacement at rupture under thermal shock

Table - 5

(The Displacement values at rupture)

SI No	Sintering Temperature (°C)	Sintering Time (hr)	Displacement at Rupture (mm)	
			+80°C	-80°C
1	600	1.0	1.8750	0.5749
2		1.5	X	0.9466
3		2.0	1.0930	0.6262
4	580	1.0	1.4460	0.7085
5		1.5	X	X
6		2.0	X	X
7	560	1.0	1.6770	0.6994
8		1.5	0.6902	0.7946
9		2.0	1.0490	X
10	540	1.0	X	1.0230
11		1.5	1.1000	0.7635
12		2.0	0.8550	0.5639

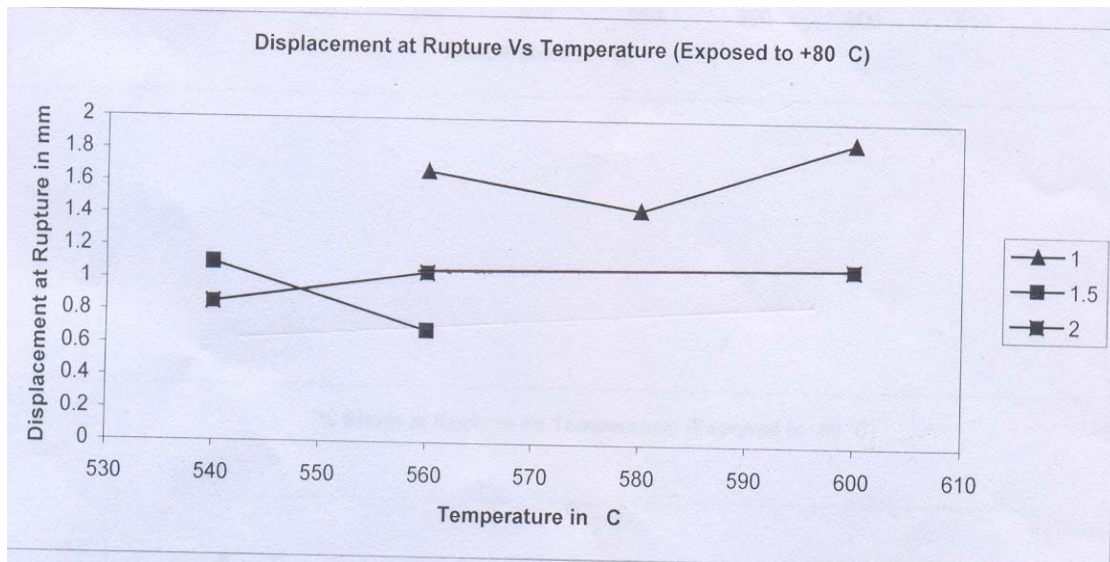


Fig No.34 - Displacement at rupture Vs Temperature as a function of Time (Exposed to +80°C)

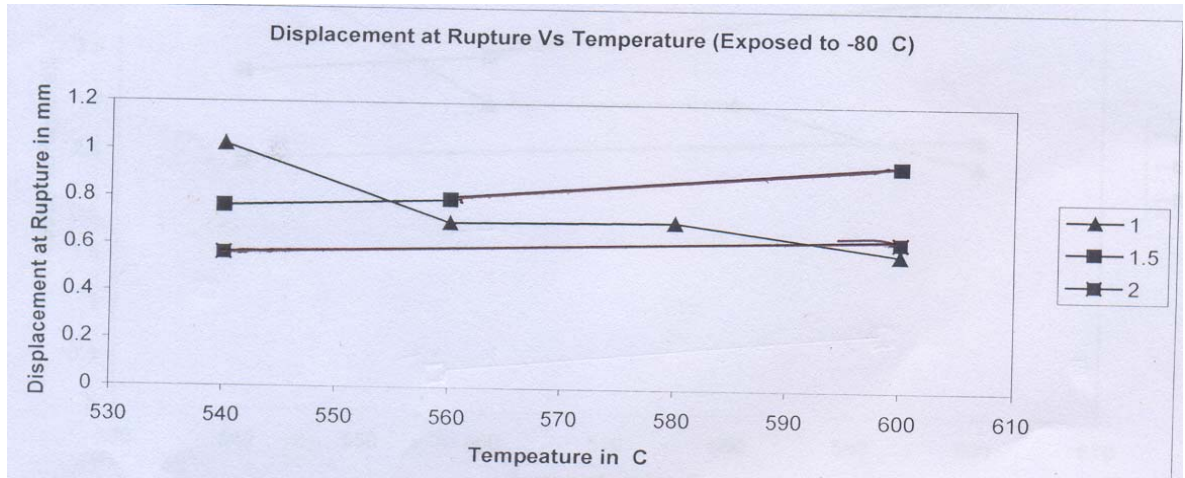


Fig No.35 - Displacement at rupture Vs Temperature as a function of Time (Exposed to -80°C)

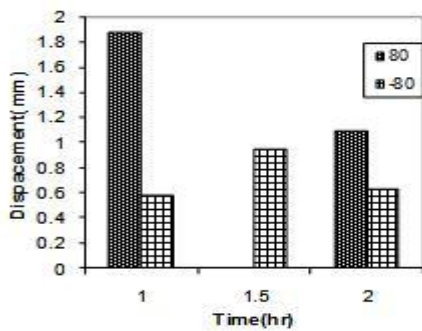


Fig no 36 : Bar diagram showing displacement at rupture V/s time at sintering temperature (600°C) for samples exposed to +80°C & -80°C.

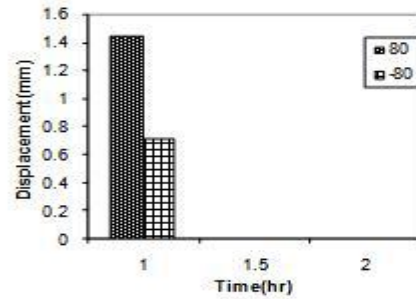


Fig no 37 : Bar diagram showing displacement at rupture V/s time at sintering temperature (580°C) for samples exposed to +80°C & -80°C.

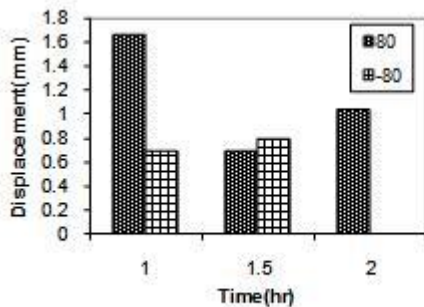


Fig no 38 : Bar diagram showing displacement at rupture V/s time at sintering temperature (560°C) for samples exposed to +80°C & -80°C.

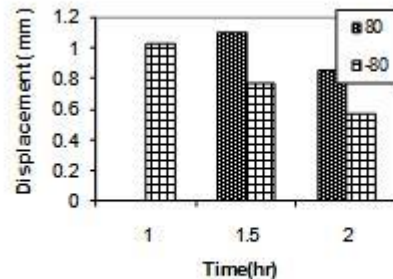


Fig no 39 : Bar diagram showing displacement at rupture V/s time at sintering temperature (540°C) for samples exposed to +80°C & -80°C.

The Displacement values, i.e. the total deformation undergone by the specimens before giving way to rupture are tabulated in table no.5. These values are plotted against time of holding at the sintering temperatures in fig no.34 and fig no.35 for the samples treated at $+80^{\circ}\text{C}$ and -80°C respectively. Fig no.36 through fig no.39 presents these values vs. time of holding at sintering temperature as bar-diagrams. The results show the following trend in general:

For samples treated at a temperature above the ambient temperature, irrespective of the sintering temperature, the total deformation undergone by the test piece is lowered with the increase of the holding time at the sintering temperature.

For samples exposed to a sub ambient temperature, i.e. -80°C , however, the trend is slightly different. While at relatively high temperature of sintering there is an increase in the extent of deformation with increase in the holding time, at relatively lower temperature, the displacement actually decreases with increase in the holding time.

In all case, concerning temperature and time, however, the extent of deformation prior to failure assume a lower value when exposed to a sub ambient temperature than the corresponding values when the specimens are exposed to an elevated temperature.

Liu, et.al [16] have concluded that the particle reinforced MMCs the mismatch in the CTE in the matrix and the reinforcement gives rise to residual stresses in the matrix during fabrication of the composite itself. In addition to this when the composite is exposed to an elevated temperature the mismatch furthers the development of residual stresses. Irrespective of the sintering temperature the interatomic diffusion gets enhanced with the increase in the time of holding at the sintering temperature. This generates a strong interface. The strong interfacial bonding so developed acts as a

constraining factor for matrix deformation [42]. The Al-SiC MMC therefore develops high residual stresses, as the redistribution of these cryogenic stresses is limited due to the increased interfacial strength and added to that plastic flow of the matrix Al is constrained [36]. This explains the decrease in the total deformation/displacement of the Al-SiCp composite in question before rupture sets-in, with the increase in the holding time of the sintering temperature at all sintering temperatures examined.

As stated earlier, when the sintering temperature is relatively high and the holding time of sintering temperatures is increased at this relatively high sintering temperatures, the total deformation /displacement values prior to rupture are increased on exposing the specimens to a sub-ambient temperature. At a sub ambient temperature the matrix Al contracts to greater extent than the reinforcements SiCp due to the mismatch in the respective CTE. This leads to the generation of residual stresses. These cryogenic stresses can be released either by the cracking of the particulate reinforcement or by the discontinuities. However there is little redistribution of these cryogenic residual stresses due to the high temperature at sintering and the longer time of holding at the sintering temperature. In this case, therefore, the only possibility of stress release is by reinforcement cracking. Mummery, et.al [42] suggest that in the case of a strong deformation, particle cracking can be considered as the only factor responsible for the increase in the ductility in the way of being the only means for cryogenic stress release. Therefore, the increase in the total deformation in this particular case may be explained by the cracking of particulate reinforcement. This phenomenon is supported by the observation put forth by L lorea, et.al. [15]. They suggested that in the initial stages of plastic deformation the increase in the load carried by the particulate reinforcement is

mainly due to progressive strain hardening of the relative ductile matrix. As the matrix strain hardening capacity is saturated (due to increase in the cryogenic residual stress in this case) relaxation of stresses result from the fracture of the particulate reinforcement which further results in the stress transfer to the near by particles causing greater particle fracture leading to the final failure of the composite. (To be ascertained by SEM micrographs)

As revealed from the data in table no.5 and the related plots (fig no34 &35 and the bar charts(fig36,37,38,39) at relatively low temperature of sintering, increases in the holding time at the sintering temperature results in the decrease in the total deformation/displacement undergone by the composite specimens prior to rupture when the specimens are exposed to a sub ambient temperature. This phenomenon is attributed to the generation of residual stress due to the mismatch in the CTE of the matrix Al and SiCp reinforcement, which cannot get redistributed due to a relatively strong interface, developed due to increase in the holding time at sintering temperature. Thus the plastic deformation of the matrix is constrained and the total percentage of displacement is limited.

4.2.4 Strain at rupture due to thermal shock

Table - 6

(The strain values at rupture)

SI No	Sintering Temperature ($^{\circ}\text{C}$)	Sintering Time (hr)	Strain at Rupture (%)	
			+80 $^{\circ}\text{C}$	-80 $^{\circ}\text{C}$
1	600	1.0	7.825	2.438
2		1.5	X	4.080
3		2.0	4.736	2.685
4	580	1.0	6.245	3.041
5		1.5	X	X
6		2.0	X	X
7	560	1.0	7.241	3.004
8		1.5	2.975	3.467
9		2.0	4.601	X
10	540	1.0	X	4.434
11		1.5	4.763	3.305
12		2.0	3.679	2.424

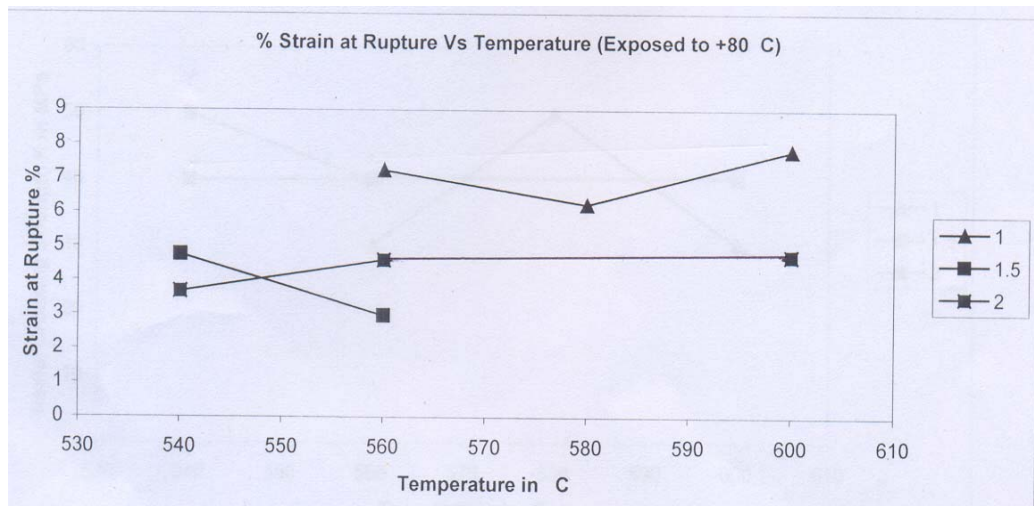


Fig No.40 Strain at rupture Vs Temperature as a function of Time (Exposed to +80 $^{\circ}\text{C}$)

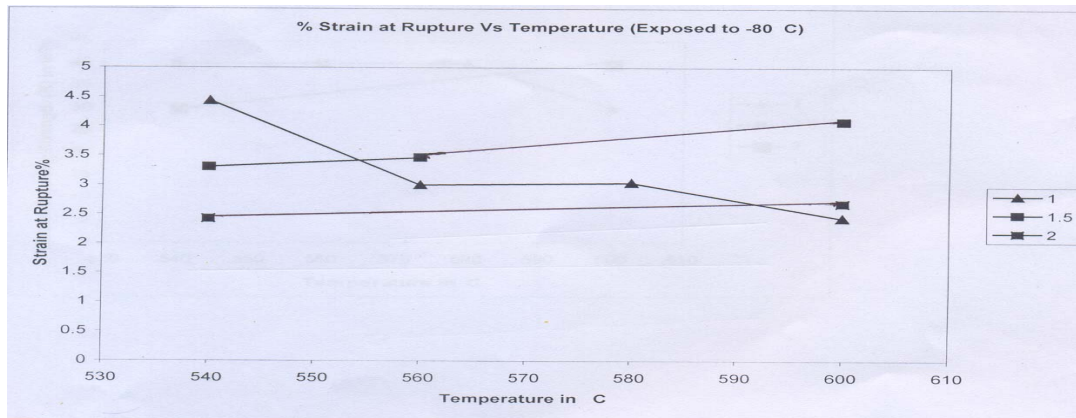


Fig No.41 Strain at rupture Vs Temperature as a function of Time (Exposed to -80°C)

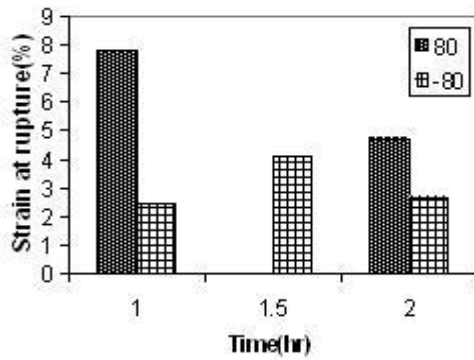


Fig no 42 : Bar diagram showing strain at rupture V/s time at sintering temperature (600°C) for samples exposed to +80°C & -80°C.

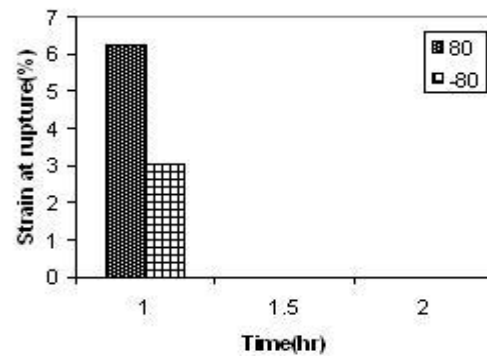


Fig no 43 : Bar diagram showing strain at rupture V/s time at sintering temperature (580°C) for samples exposed to +80°C & -80°C

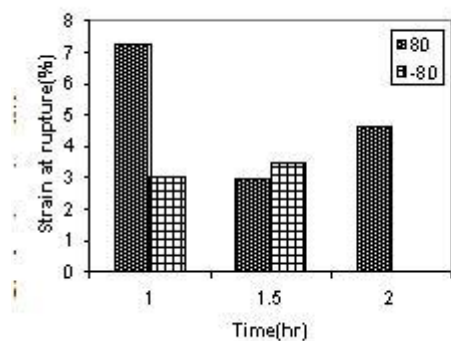


Fig no 44 : Bar diagram showing strain at rupture V/s time at sintering temperature (560°C) for samples exposed to +80°C & -80°C.

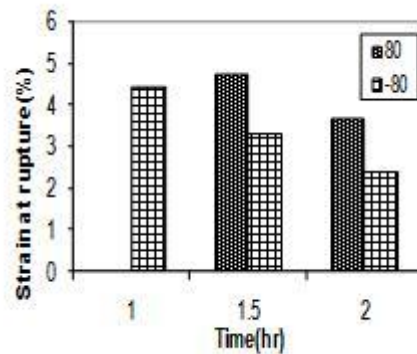


Fig no 45 : Bar diagram showing strain at rupture V/s time at sintering temperature (540°C) for samples exposed to +80°C & -80°C

The percentage strain at rupture values undergone by samples due to the treatment at an elevated temperature of $+80^{\circ}\text{C}$, sintered at different temperatures and held at the sintering temperature for various length of time are tabulated in table no.6. These values are plotted against temperatures for different holding time in fig no.40 and fig no.41. Fig no.42 through fig no.45 show these experimental findings in the shape of bar diagrams.

Strain is the change in length per unit length of the material exposed to the load. Greater is the extent a material can be strained, greater is its ductility, and greater is its ability to deform before cracking under the applied load. Keeping this in mind it may be appreciated that the percentage of strain due to thermal shock as recorded in table no. 6 has direct links with the total displacement undergone by the material before rupture.

The percentage strain variations exhibit the same trend as those exhibited by the total deformation/displacement and can be attributed to similar factors as discussed earlier in the case displacement variation.

A measure of the extent to which a material will deform before fracture gives its ductility. Besides the reduction in area of the cross section at fracture, the conventional measure of ductility is the engineering strain at fracture i.e. the elongation or change in axial length divided by the original length or simply the percentage strain. Thus the percentage strain in rupture is an important material property to be considered while designing an engineering component. A material characterized by lower values the percentage strain at fracture will generate an engineering component which will give way under load catastrophically without giving warning where as material exhibiting higher values will get deformed as a consequence of the applied load, give a warning

and then fail. In light of the above one may take about toughness of the material. The key to toughness is a good combination of strength and ductility. A material with high strength and high ductility will have toughness than one with low strength and high ductility.

It is thus interesting to note the following, considering the results as obtained in this work concerning both, the stress at fracture or simply the capacity of the material to absorb energy before fracture and the percentage strain or ductility or simply the ability of the material to deform plastically before fracture. Exposure to an elevated temperature, that of the ambient, is not much damaging for short-term use of the material when the sintering temperature is relatively high.

Exposure to a sub ambient temperature is not much damaging for short-term use of the material when the sintering temperature is relatively low.

However, when long term use is concerned either of the two i.e. ability to absorb energy and ability to deform plastically before rupture, or both of them do not exhibit good results when exposed to thermal shock at an elevated temperature at an/or sub ambient temperature. This will result in relatively lower values of toughness restricting the use of the material fabrication of load bearing engineering components.

It is further noted that for all cases of temperature of sintering and time of holding at the sintering temperature, an exposure to the sub ambient temperature yields a lower value of the total displacement at rupture than the exposure to an ambient temperature. This may be attributed to the difference in CTE of the matrix and the reinforcement bringing in the development of residual stresses responsible for restricting the plastic

flow of the matrix there by resulting in lower total displacement values before fracture set in.

Radial Crushing Strength 'K' under the influence of thermal shocks

Table - 7

(The radial crushing strength)

Sl No	Sintering Temperature (°C)	Sintering Time (hr)	Calculated Radial Crushing Strength(MPa)	
			+80°C	-80°C
1	600	1.0	30	30
2		1.5	X	40
3		2.0	40	40
4	580	1.0	50	40
5		1.5	X	X
6		2.0	X	X
7	560	1.0	30	40
8		1.5	40	40
9		2.0	40	X
10	540	1.0	X	40
11		1.5	50	40
12		2.0	40	30

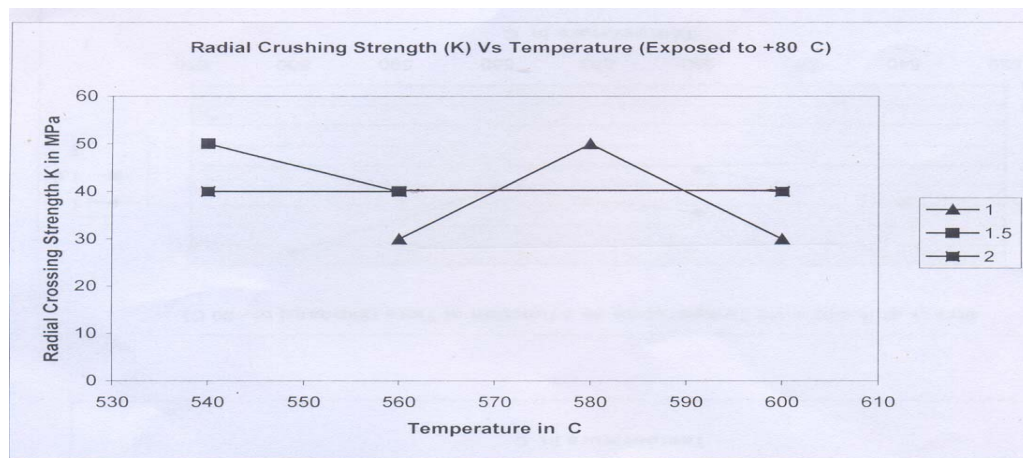


Fig No.46 Radial Crushing Strength Vs Temperature as a function of Time (Exposed to +80°C)

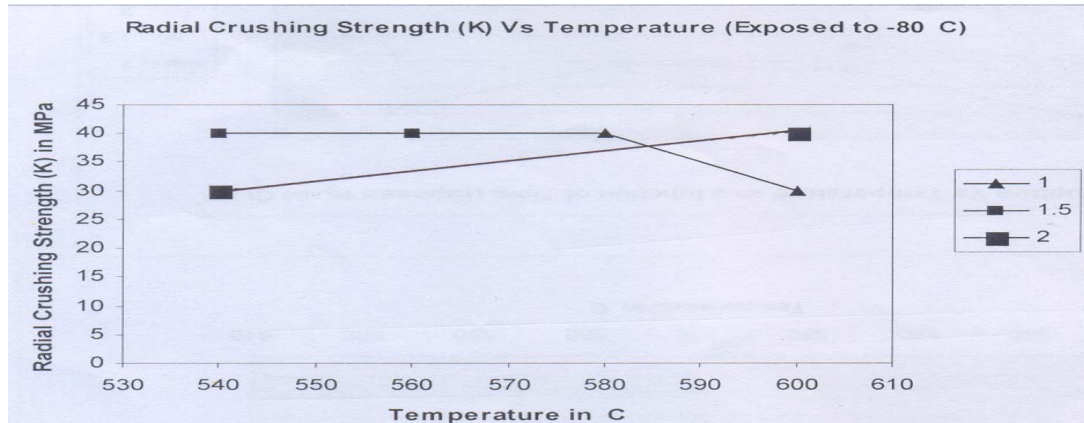


Fig No.47 Radial Crushing Strength Vs Temperature as a function of Time (Exposed to -80°C)

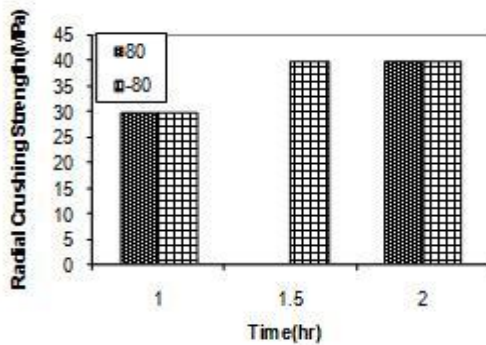


Fig no 48 : Bar diagram showing radial crushing strength V/s time at sintering temperature (600°C) for samples exposed to +80°C & -80°C.

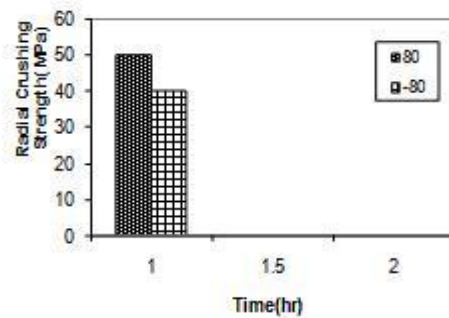


Fig no 49 : Bar diagram showing radial crushing strength V/s time at sintering temperature (580°C) for samples exposed to +80°C & -80°C

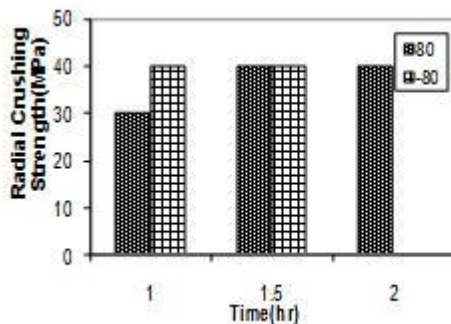


Fig no 50 : Bar diagram showing radial crushing strength V/s time at sintering temperature (560°C) for samples exposed to +80°C & -80°C.

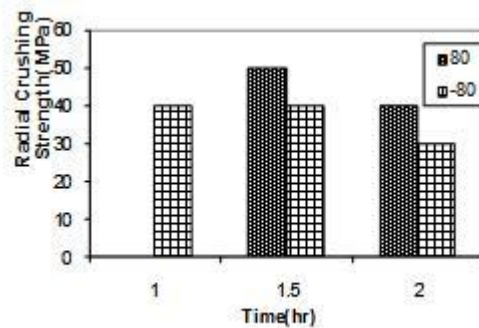


Fig no 51 : Bar diagram showing radial crushing strength V/s time at sintering temperature (540°C) for samples exposed to +80°C & -80°C

Radial Crushing Strength, which is calculated to the nearest 10 MPa, is presented in table no. 7 for samples sintered at different temperature and held at the respective sintering temperature for different length of time. These are plotted against temperature of sintering for various holding times in fig no.46 and fir.no.47 for samples exposed to +80⁰C and -80⁰C respectively. The K values are also presented in the shape of bar diagrams in fig no. 48 through fig. No. 51 in order to just make an comparative study, when the specimen are exposed to both a temperature above the ambient (+80⁰C) and that below the ambient (-80⁰C).

The Radial Crushing Strength test is used to determine the strength characteristics of hollow cylindrical test specimens. The related ASTM standard, B 939-05 clearly states that these test results can only be used for comparison with data from the test specimens of like materials and similar dimension. The standard further states that it does not address to the safety concerns, if any, associated with its use. It also states that the radial crushing strength of a material is approximately twice it ultimate tensile strength.

The experimental data and the plots including the bar-diagrams revealed that the variation of the 'K' values for samples sintered at different temperature and held at the respective sintering temperature for different length of time follow a similar trend as the stress of the specimen when exposed to both an elevated and a sub-ambient temperature. Noting that the 'k' values represent the strength characteristics of the material as does the stress, its variation trend can be attributed to similar reasons as stated in case of stress variations. How ever, a close look at the experimental 'k' values will reveal that in general .The 'k' values of the specimen are almost identical when

exposed to the thermal shock due to either a rise in the temperature or a fall in the temperature below that of the ambient.

4.3 B. Assessment and Evaluation Based on SEM Micrograph Studies

Extensive micrographs studies have been carried out using SEM (JSM 6480 LV). An attempt has been made to explain the failure mode as a result of thermal shock in terms of interfacial bonding, residual stresses, decohesion, matrix dislocations, etc., with the aid of the micrographs. Some of the representative micrographs are presented in Micrograph No. 1 through Micrograph No. 10 and discussed at length.

The Interface (boundary between the matrix and the reinforcement) in a MMC is a porous, non-crystalline portion in the composite in comparison to the metal matrix or the ceramic reinforcement. Thermal effects, i.e., when the MMC is exposed to either an elevated temperature or (above that of the atmosphere) a sub-ambient temperature, brings in thermal stresses due to a difference in the CTE of the Metal matrix and the ceramic reinforcement. In the present case thermal effects induce tensile stresses in the Al-matrix and compressive stresses in the SiC_p reinforcement due to the differences in the CTE of the both.

The state of residual stresses, thus generated, is mostly dynamic. These relax by the phenomena as presented below:

- (i) Interface Sliding
- (ii) Decohesion
- (iii) Plastic Strain

(iv) Micro and Macro Cracking and

(v) Particulate Breaking / Cracking

Relaxation of residual stresses in Al / SiC_p MMC_s over long periods of time has been observed at room temperature [58]. Thermal cycling by reversing between high or low temperatures including sub-ambient temperature and the room temperature can also modify the residual stresses. Stresses induced due to the differences in the CTE of the matrix and the reinforcement may impart plastic deformation to the matrix thereby resulting in a reduction in the residual stresses. Thermal mismatch strains also may quite often develop cracks in the matrix as a result of the large tensile residual stresses, again resulting in a relaxation of the residual stresses.

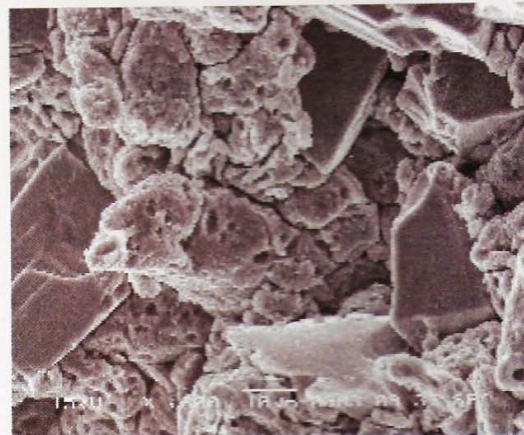
Residual stresses are readily relaxed at the porous and non-crystalline interface. As a result when the particle density is high, i.e., interface availability is plenty, failure is due to the formation and propagation of cracks at the interfacial region. This process of failure proceeds by the nucleation of voids and subsequent coalescence of the voids for formation and propagation of the crack leading to failure. On the other hand when the particle density is low, i.e., in regions, which are particle starved, meaning that the availability of interface is limited, particle failure is predominating.

The representative micrographs as obtained through SEM analysis are presented in Micrograph No. 1 through Micrograph No. 10.

Micrograph No. 1 & 2 reveal Matrix as well as particle fracturing. The exposure to -80°C makes the ductile Al matrix brittle leading to failure because of reduced or no relaxation processes (atomic migration, atomic rearrangement, stress/strain relaxation).



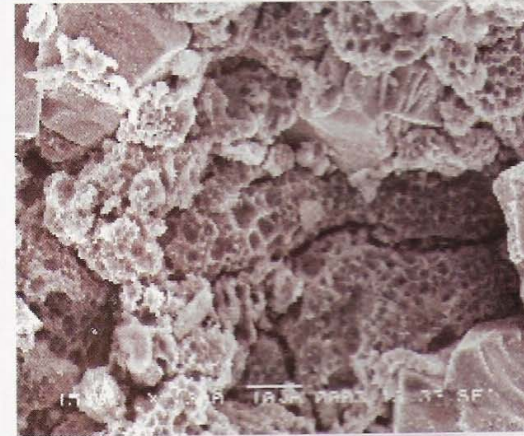
Micrograph No. - 1
Temp - 600°C, Time - 1.5hrs, Treatment - "-80°C"



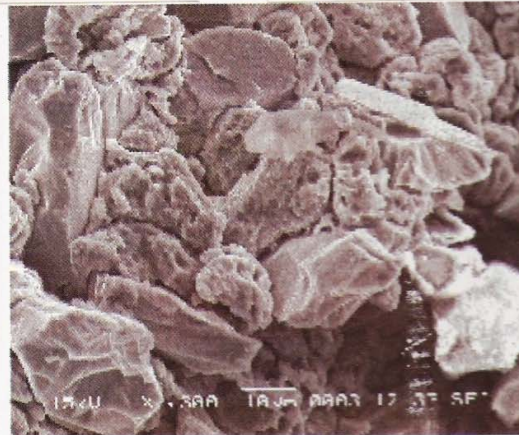
Micrograph No. - 2
Temp - 560°C, Time - 1.5hrs, Treatment - "-80°C"



Micrograph No. - 3
Temp - 540°C, Time - 1hr, Treatment - "-80°C"



Micrograph No. - 4
Temp - 540°C, Time - 2hrs, Treatment - "-80°C"



Micrograph No. - 5
Temp - 560°C, Time - 1.5hrs, Treatment - "-80°C"

Micrograph No. 3 reveals the matrix damage in the form of an outcrop resulting in a crumbling of the Matrix. This might have resulted from a contraction of the matrix due to the exposure to the sub-ambient temperature.

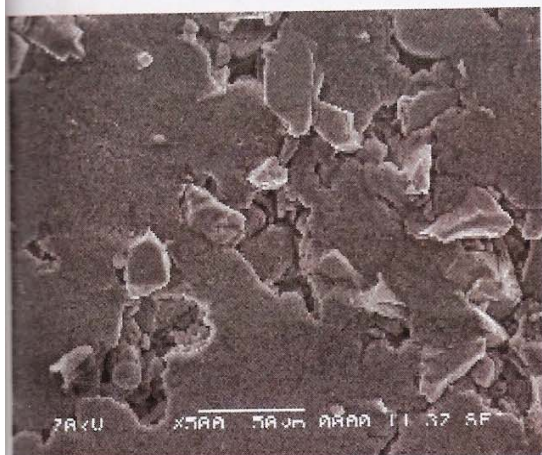
Micrograph No. 4 shows the effect of the outcrop due to contraction of the matrix as a result of an exposure to the sub ambient temperature. The outcrop leads to coalescence of micro voids effectively. This coalescence of the micro voids gives way to the generation of potential macro-voids, which in its turn lead to a reduced threshold energy for the cracks to be generated for subsequent propagation.

An analysis of micrograph no. 5 helps to note that the points as noted against micrograph No. 4 leading to the generation of cracks are less global. These revelations i.e., the outcrop leading to the crumbling of the matrix is not being global, is more damaging in nature.

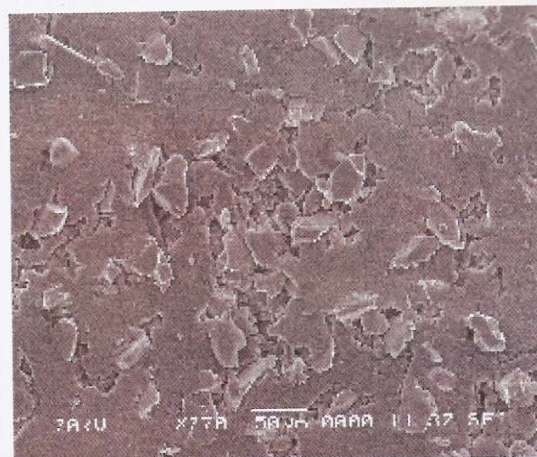
Micrograph No. 6 and No. 7 again reveal a matrix failure. Here incomplete sintering has resulted in improper anchorment of particulates. Thus particles strengthening are not attained and therefore exposure to the elevated temperature (+80⁰C) leads to matrix failure. This is because here in this case stress is not being transferred to the particles due to the weak bonding between the matrix and the reinforcement.

Micrograph No.8 shows interfacial failure due to an exposure to the sub-ambient temperature (-80⁰C). Here the interfacial stress transfer seems to be more effective.

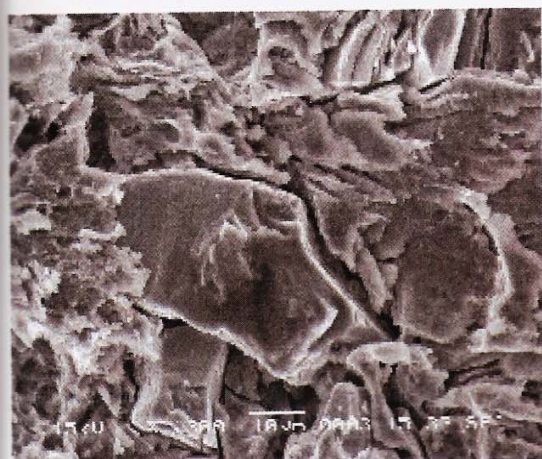
Micrograph No. 9 and Micrograph No. 10 show predominating particle failure. This may be due to the transfer of stress generated due to cryogenic conditioning (-80⁰C) from matrix to the particulates. These micrographs clearly show that the



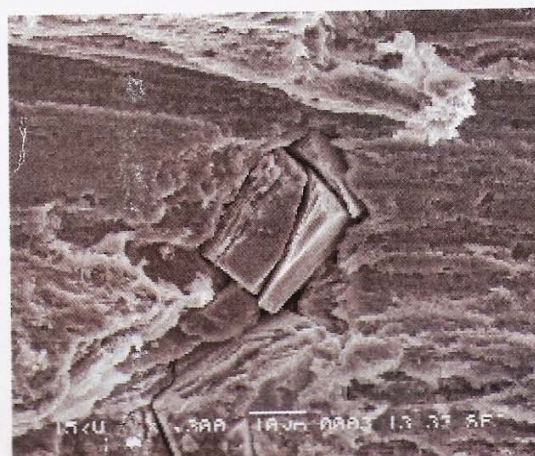
Micrograph No. - 6
Temp - 580°C, Time - 1.5hrs, Treatment - "+80°C"



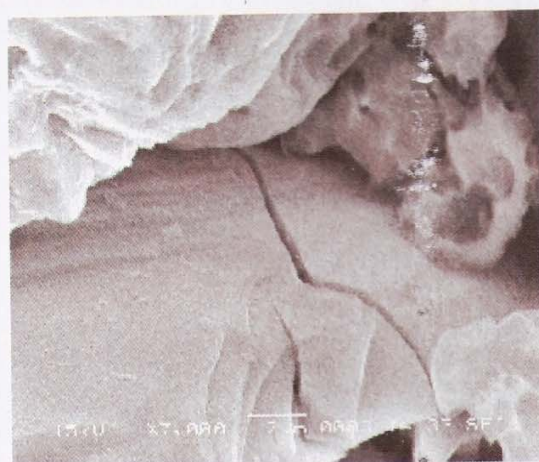
Micrograph No. - 7
Temp - 560°C, Time - 1hr, Treatment - "+80°C"



Micrograph No. - 8
Temp - 580°C, Time - 1hr, Treatment - "-80°C"



Micrograph No. - 9
Temp - 540°C, Time - 2hrs, Treatment - "-80°C"



Micrograph No. - 10
Temp - 600°C, Time - 2hrs, Treatment - "-80°C"

concerned regions are particle stard regions making limited availability of the interface which in turn encourages particle failure as a result of the stress transfer from the matrix to the particulates.

To sum up, as revealed through the micrographs, in general, when the thermal shock is due to the exposure to an elevated temperature, the dominating failure mode is cavity generation. At this high temperature inter- diffusion is high resulting in strong bonding. Therefore, the failure in this case is primarily due to the generation of cavities, i.e., discontinuities, at the interface.

However, in general, when the thermal shock is due to an exposure to a sub ambient temperature, the dominating failure mode is interfacial failure and/or matrix damage.

CHAPTER 5

CONCLUSION

The following conclusions are drawn on the basis of the results obtained and discussions made :

- 1) Residual stresses as a result of thermal mismatch are responsible for the failure of the MMCs.
- 2) Thermal shock at an elevated temperature is less damaging for short-term use of the MMCs when the sintering temperature is relatively high.
- 3) At relatively low sintering temperature for short-term use thermal shocks due to sub ambient temperature are less damaging.
- 4) For long term use for all temperatures of sintering, the thermal shock, whether it is due to elevated temperature or sub ambient temperature is damaging, in the way of affecting either the strength properties or the ductility or the both simultaneously.

BIBLIOGRAPHY

1. Ashby, M.F., Materials selection in Mechanical Design, Third Ed. ed; Oxford, 2005.
2. Mathews, F.L. and Rawlings, R.D., Composite Materials; Engineering and Science, Chapman and Hall, 1994.
3. Fundamentals of Metal-Matrix composites, copyright, 1993. by Butterworth-Neimann.
4. Alcan Aluminium Corporation, Product Brochure, 1991, San Diego, CA.
5. Ray, P.K., Bera, T. Ranjan, R., Mohanty, U., Vadhera, S., Ray, B.C., Proc. Of Conf. On Emerging Trends in Structural Materials, NIT, Rourkela, 2003.
6. Smith, W.F. " Principles of Materials Science and Engineering," 3rd ed. (Mc Grow Hill, New York 1996)
7. Kalam, A.P.J.A., Tiwari, A. " wings of five" (Universities Press, New Delhi, 2003)
8. Jagnes, E, Schoutens and Kaman Tempo, Introduction to Metal Matrix Composite Materials, (DoD Metal Matrix Composites Information Centre, 1982); 2-2.
9. IBID, 3-1.
10. Lloyd, D.J., Acta Metal Mater, 1991; 39; 59.
11. Whitehouse, A.F. Clyne, T.W. Acta Metall Mater, 1993; 41:1701.
12. Ribes, H., Da Silva, R., Suery, M., Bretheau, T., Mater Sci Technol, 1990, 6:621.
13. Song, S.G., Ghi, N., Gray III, G.T. and Roberts, J.A. Metall Mater. Trans. A27, 1996, 3739
14. Qin, S., Chen, C., Zhang, G., Wang, W., and Wang, Z., Material Sci. Eng., A272, 1999, 363.
15. Llorea, J., Gonzalez, C., and J. Mech. Phys. Solids, 46, 1998, 1.
16. Liw, cheng., Qin. Shuyi., Zhang, Guoding. and Naka, Masaaki, Mat. Sc. and Engg. A332, 2002, 203-209.
17. Kopp, M.W., and Jien, J.K. " Interdiffusional Instability in High Temp. Metal Matrix Composites, " (paper presented at the 9th Riso International Symposium, Roskilde, Denmark, 5-9 Sept., 1988)
18. Srivatsan, T.S., editors, Rapid Solidification Technology: an Engg. Guide. Lancaster, PA: Technomic publishing Inc; 1993, 603-700.

19. Kocjak, M.J., Khatri, S.C., Alison, J.E., Bader, M.G., In: Suresh, S. Mortensen, A., Needleman, A., editors; Fundamentals of Metal Matrix Composites, Boston, MA: Butterworth- Heinemann; 1993, 297-317.
20. Mc Guire, P.F., Aluminium Composites come in for a landing, Machine Des;1992; 64:71-4.
21. Hunt Jr, W.H., Cook, C.R., Sawtell, R.R., cost effective high-performance powder metallurgy aluminium matrix Composites for automotive applications, 1991, Annual SAE Congress, Paper no. 91D834, Detroit, Michigan; 1991.
22. Lloyd, D.J., Int. Mater. Rev., 1994; 39; 1-23.
23. Sugimura, Y, Suresh, S., Effects of SiC content on fatigue crack growth in aluminium alloys reinforced with SiC particles. Metall Trans, 1992; 23A: 2231-42.
24. Liaw, P.K., Logsdon, W.A., Engng. Fract. Mech., 1986; 24:637-45.
25. Davidson, D.L. Engng. Fract Mech., 1989; 33:965-77.
26. Manoharam, M., Lewandowski, J.J., Acta Metal, 1990; 38(3): 489-99.
27. East, W.F. Metal-Matrix Composites take-off, Mater. Engng; 1998, March: 33-6
28. DeMeis, R. New life for Aluminium. Aerospace Am 1989; March: 26-8.
29. Nair, S. V., Tien, J.K., Bates, R.C., Int. Metals Rev. 1985; 30 (6): 285-97:
30. Mc Donels, D.L., Metall Trans., 1985; 16A; 1105-15.
31. Willis, T.C., Metals Mater, 1988; August: 485-9.
32. Davis, L.C., Allison, J.E., Metall Trans.,1993; 24 A : 2487 – 94.
33. Vogelsang, M., Arsenault, R. J., Fisher, R.M., Metall. Trans., 1986; 17A: 379 – 89.
34. Sinclair, I. Grepson, P.J., Mater. Sci. Technol. 13., 1997, 709.
35. Looney, L., and O' Donnell, G., Material Science and Engg., A 303, 292 – 301, 2001.
36. Srivastan, T.C., Meglet, Al-Hairi, Smith, C., and Petraoli, M., Mat. Sc. And Engg., A 346, 91-100.2003.
37. Chawla, N., Williams, J.J., Saha, R., Journal of light metals, 2, 2002, 215-227.
- 37A. ASTM B09, Metal powder Industries Federation(MPIF),105 College Rd East.Princeton.NJ 08540-6692,USA
38. Tham, L.M., Gupta, M., Cheng, L., Acta mater. 49, 2001, 3243.
39. Iseki, T., Kameda, T., Maruyama, T., J. Mater. Sci, 19, 1984, 1692.

40. Warren, R., Anderson, C.H., Composites, 15, 1984, 101.
41. White house, A.F., Clyne, J.W., Acta. Metal. Mater. 41, 1993, 1701.
42. Mummery, P.M., Derby, B, Buttle, D.J., Seruby, C.B., Proceedings of the second European Conference on Advanced Materials and processes, University of Cambridge, U.K., July., 22-24, 1991, Institute of Materials, London, U.K., 1992, P. 441.
43. Tham, L.M., Gupta, M., Cheng, L., Materials Science and Engg. A354, 2003, 369-376.
44. Lenel, F.V., Powder Metallurgy, Princeton, NJ: Metal Powder Industries Federation, 1980.
45. Harrington; W.C., Flowers, R.H., and Hudson, S.P., U.S. Patent no. 4, 223, 075, Sept. 16, 1980.
- 45A. Fundamentals of Metal Matrix Composite Ed. By Suresh,S., Mortensen, A., Needleman, A., Chapter-1 P: 3-22, Butterath Heinemann, Uk.1993
- 45B Recycling of MMCs & Production of metallic foams by Gergely,V.,Degischer, H.P., Clyne,T.W.,(Comprehensive Composite Material-3,Metal Martix Composite)
46. Kennedy, C.R., Satellite Symposium 2 on Advanced Structural Inorganic composites of the 7th International Meeting on Modern Ceramics Technologies, 691-700, London and New York; Elsevier Science, 1991.
47. Pennander, L., and Anderson, C.H., Metal Matrix Composites Processing, Microstructure and Properties, International Symposium or Materials Science, 575-580, Roskilde, Denmark, 1991.
48. Tsunekawa, Y., Okumiya, M., Numi, L., and Yoneyama, k., I. of Material Science Lett. 6: 191-193, 1998.
49. Andress, R.M., and Mortensen, A., Metall. Trans., 22A, 2903-2915, 1991.
50. Rohatgi, P.K., Asthana, R., Das, S., Intern. Metals Rev., 31, 115-139, 1986.
51. Skibo, M.D., and Schuster, D.M., U.S., Patent no. 4, 786, 467, November 22, 1988.
52. Xiao, P., and Derby, B., British Ceramic proceedings, 153-159, 1991.
53. Sahoo, P., and Koczak, M.J., Mater. Sc. and Engg., A- 144. 37-44, 1991.
54. Rawal, S. and Misra, S., Sample conf. proceedings, 317-326, 1990.
55. Gunashekhar, J.S., and Hoshino, S., Annals In. Inst. Prod. Eng. Res. (CIRP),29; 141, 1980.

56. Syu, D.G.C., and Ghosh, A.K., A Comparison of forging limits of several aluminium matrix composites, (submitted to Metal. Trans. A., 1992.
57. Sritharan, T., Xia, K., Heathcock, J., Mihelich, J., and Metal & Ceramic Matrix Composites: Processing, Modeling & Mechanical Behavior, 1990
58. Witners, P.J., Stobbs, W.M. and Pedersen, O.B., Acta Metall., 37, 3061-84; 1989.